Gauge theory of the normal state of high-T_c superconductors

Patrick A. Lee
Department of Physics, Massachusetts Institute of Technology, Cambridge, Massachusetts 02139

Naoto Nagaosa
Department of Applied Physics, University of Tokyo, Tokyo 113, Japan
(Received 20 February 1992)

Starting with the one-band t-J model and using the slave-boson method to enforce the constraint of no double occupations, we examine fluctuations about the uniform resonating-valence-bond mean-field solution. We restrict our attention to a temperature region where the bosons are not Bose condensed. The important low-energy fluctuations are described by gauge fields that are related to fluctuations in the spin chirality. The fermions and bosons are strongly coupled to the gauge field, leading to a transport time of order $\hbar/k_B T$, in agreement with experiment. The model also exhibits a Fermi surface with area $1-x$, where x is the dopant concentration, consistent with the Luttinger Theorem, but the low-lying excitations have a decay width much larger than its energy, in violation of Landau's criterion for a Fermi-liquid state. Other experimental implications of this model and the possibility of a direct measurement of the chirality fluctuations are discussed.

I. INTRODUCTION

After several years of intense experimental and theoretical studies of the copper-oxide superconductors, there is now a consensus that these materials should be described as strongly correlated electronic systems. The undoped parent compound, such as La_2CuO_4, is understood to be a Mott-Hubbard insulator, with $S=\frac{1}{2}$ local moment on the copper sites which are antiferromagnetically ordered below 200 K or so. Upon doping with holes in the copper-oxygen plane, the long-range-ordered antiferromagnet (AF) is replaced by short-range order and superconductivity emerges as the ground state. The magnetism has been extensively studied by neutron, μSR, and NMR techniques.[1] While the origin and the nature of the superconductivity remains a puzzle, much attention has been focused on the normal-state properties of the doped materials at a temperature above the superconducting T_c. As emphasized early on by Anderson,[2] the normal-state properties are anomalous in the sense that they do not fit in with conventional Fermi-liquid theory. One of the earliest anomalies is the linear T dependence of the resistivity. Optical-conductivity measurements[3] have revealed a narrow Drude-like peak with a width which is of order $2k_B T$, so that the linear T resistivity is now understood to be due to a scattering rate that is linear in T. Recent microwave measurement of the quasiparticle contribution to the conductivity below T_c have shown that the scattering rate decreases greatly below T_c.[4,5] This provides strong evidence that the anomalous scattering rate is electronic in origin and not due to scattering by some soft phonon.

The spectral weight of the Drude peak only of the conductivity is found to be proportional to the dopant concentration x, and can be fitted by x/m, where $m \approx 2m_e$.[3] The Hall effect has an anomalous temperature dependence which is sensitive to disorder scattering in the sample. Very recently the Hall data have been successfully analyzed by the introduction of an additional temperature-dependent scattering time.[6] Even though the microscopic origin of this scattering time remains unclear, a carrier number which is of order x is extracted by this analysis. Thus, the transport data can apparently be understood as being due to x doped holes with a modest mass and some anomalous scattering rate. This simple picture was shattered by the availability of high-resolution angle-resolved photoemission data[7] which indicate the existence of a Fermi surface, with an area consistent with band calculations. Since band theory is consistent with Luttinger theorem, this means that the Fermi surface area contains $1-x$ electrons. The important point is that the local moment on the copper sites, which are localized in the half-filled Mott-Hubbard insulator, is now counted as part of the Fermi surface area when the system is doped to a metallic state. It is now apparent that the normal state is a complicated correlated state which simultaneously displays the localized and extended nature of the copper moment. It is not at all clear that this state is describable using conventional Fermi-liquid theory.

On the theoretical front, Anderson[2] and later Zhang and Rice[8] have argued strongly that the basic physics of the copper-oxygen plane can be described by a one-band Hubbard model. We shall adopt this point of view here. Furthermore, we take the large-U limit of the Hubbard model, which reduces to the t-J model. Anderson has introduced the idea of the resonating valence bond (RVB) to describe the short-range AF state. Baskaran, Zou, and Anderson[9] introduced a mean-field decoupling of the exchange term. They produced a mean-field solution in which a spinon Fermi surface emerges. A number of other more elaborate mean-field solutions have been introduced and by now the mean-field theory both at half-filling[10-13] and away from half-filling[14-18] has been considerably clarified. Examples include the flux phase[10] and the commensurate flux[17-20] phase which breaks time-reversal symmetry and parity. The latter is related to the proposal of fractional statistics[21] and anyon superconduc-

tivity.[22,23] It would seem a hopeless task to determine from first principles which of the many proposed solutions is realized as a solution to the t-J model. In this paper we set for ourselves a rather more modest goal. We want to ask the question: Given a mean-field solution and by including fluctuations around it, can we obtain a description of physical quantities which are consistent with the rather severe constraints set by experiments?

Baskaran and Anderson[24,25] recognized that fluctuations about the RVB mean-field solution are naturally gauge theories. This point was elaborated in a paper by Ioffe and Larkin,[26] and we shall draw heavily from the results of this work. We find that, even though the spin and charge degrees of freedom are separated on the mean-field level, they are strongly coupled by the gauge field. In order to reproduce the photoemission data, we need a mean-field theory with a spinon Fermi surface which obeys Luttinger's theorem. This leads us to consider the uniform RVB state.[15] A short version of this work was published earlier.[27] One of our main results is that a linear T resistivity emerges due to scattering by gauge field fluctuations. A mathematically related though physically distinct mechanism for linear T behavior is given by Ioffe and Wiegmann.[28] Ioffe and Kotliar[29] have also published a work which is very closely related to the present one.

II. THE MODEL LAGRANGIAN

We shall begin with the t-J model defined on a square lattice

$$H=-t\sum_{i,j,\sigma}c_{i\sigma}^{\dagger}c_{j\sigma}+J\sum_{i,j}(\mathbf{S}_i\cdot\mathbf{S}_j-\tfrac{1}{4}n_in_j)\ , \tag{2.1}$$

where $\mathbf{S}_i=\frac{1}{2}c_{i\alpha}^{\dagger}\boldsymbol{\sigma}_{\alpha\beta}c_{i\beta}$, $n_i=\sum_\sigma c_{i\sigma}^{\dagger}c_{i\sigma}$, and the sum over ij is over the nearest neighbor. Equation (2.1) is subject to the important constraint that a given site cannot be occupied by more than one electron. The constraint is conveniently implemented using the slave-boson method:[30–32]

$$c_{i\sigma}=f_{i\sigma}b_i^{\dagger}\ , \tag{2.2}$$

where $f_{i\sigma}$ is a fermion operator that carries the spin label and $b_i^{\dagger}$ is a boson operator that can be interpreted as creating a vacancy. The constraint of no double occupancy is now replaced by

$$\sum_{i,\sigma}f_{i\sigma}^{\dagger}f_{i\sigma}+b_i^{\dagger}b_i=1\ , \tag{2.3}$$

which can be implemented in a functional integral formula over a complex b field and a Grassmann f field with the integration over an additional field λ_i on each site,

$$Z=\int d\lambda_i db_i db_i^{*}df_{i\sigma}df_{i\sigma}^{*}\exp\left[-\int_0^{\beta}(\mathcal{L}_0+H)d\tau\right]\ ,$$

where

$$\mathcal{L}_0=\sum_{i,\sigma}f_{i\sigma}^{*}\left[\frac{\partial}{\partial\tau}-\mu\right]f_{i\sigma}+b_i^{*}\frac{\partial}{\partial\tau}b_i +i\lambda_i(f_{i\sigma}^{*}f_{i\sigma}+b_i^{*}b_i-1)\ , \tag{2.4}$$

$$H=-t\sum_{i,j,\sigma}f_{i\sigma}^{*}f_{j\sigma}b_ib_j^{*}-\frac{J}{2}\sum_{i,j,\sigma,\sigma'}f_{i\sigma}^{*}f_{j\sigma}f_{j\sigma'}^{*}f_{i\sigma'}\ . \tag{2.5}$$

A boson-boson interaction term has been dropped as being small (of order x^2) in the rewriting of the J term. Equation (2.5) leads naturally to the mean-field decoupling[15]

$$\chi_{ij}^{(0)}=\sum_{\sigma}\langle f_{i\sigma}^{\dagger}f_{j\sigma}\rangle\ . \tag{2.6}$$

Alternatively, the same term can be written as

$$J\sum_{i,j}(f_{i\uparrow}^{\dagger}f_{j\downarrow}^{\dagger}-f_{i\downarrow}^{\dagger}f_{j\uparrow}^{\dagger})(f_{j\downarrow}f_{i\uparrow}-f_{j\uparrow}f_{i\downarrow})\ ,$$

which would lead to the decoupling[9]

$$D_{ij}=\langle f_{i\uparrow}f_{j\downarrow}-f_{i\downarrow}f_{j\uparrow}\rangle\ . \tag{2.7}$$

At half-filling, there exists an SU(2) symmetry[12] (an absence of a down spin is equivalent to an up spin when there is exactly a single fermion per site), so that the two decouplings are equivalent. For finite x, the two decouplings are distinct. For the bulk of this paper we shall treat the decoupling χ_{ij} while assuming that $D_{ij}=0$. There are two rationales for this. First, it is convenient formally to extend the spin sum to a sum over N degrees of freedom, and perform a large-N expansion. In this case it is clear that χ_{ij} scales as N and there is no simple way of defining D_{ij}. Indeed, Grilli and Kotliar[15] have found that, in the large-N limit, the mean field $\chi_{ij}^{(0)}\neq 0$, $D_{ij}=0$ is stable for some intermediate doping concentration $x\approx J/t$. Secondly, if we treat the $N=2$ case in the saddle-point approximation, we expect for intermediate doping that $\chi_{ij}^{(0)}\neq 0$ below a temperature of order J, while D_{ij} may develop d-state symmetry at a lower temperature,[14] so that there should be a temperature range where $\chi_{ij}^{(0)}\neq 0$ but $D_{ij}=0$. Schematically the mean-field phase diagram may look like that shown in Fig. 1. There are four different regimes. Below the solid line $\chi_{ij}^{(0)}\neq 0$ and, when D_{ij} is d-state symmetric, we have a uniform RVB state. In region I, $\langle b\rangle\neq 0$ and we have a Fermi-liquid phase, quite similar to that which appears in the heavy-fermion problem. This region has been treated by Grilli and Kotliar.[15] In region II, $D_{ij}\neq 0$ but $\langle b\rangle=0$. We shall

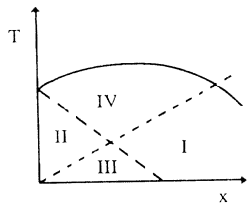

FIG. 1. Schematic slave-boson mean-field phase diagram of the t-J model. The solid line denotes the onset of the uniform RVB state. The dotted line denotes the mean-field Bose-Einstein condensation temperature of the boson while the dashed line denotes the onset of pairing of the fermion operators. The four regions are (I) Fermi liquid, (II) spin-gap phase, (III) superconductor, and (IV) strange metal phase.

refer to this as the spin-gap phase because a gap appears in the spin excitation spectrum. In region III, both $D_{ij}\neq 0$ and $\langle b\rangle\neq 0$ and when D_{ij} is d-state symmetric, we have a superconductivity phase where $\langle c_{i\uparrow}c_{j\downarrow}-c_{i\downarrow}c_{j\uparrow}\rangle\neq 0$. In region IV, $\langle b\rangle=0$ and $D_{ij}=0$. This is the region we concentrate on in the present work and we shall refer to this as the "strange metal" phase. Since it lies above the superconductivity phase, we interpret this to be the normal phase of the superconductor. This schematic phase diagram is expected to break down for small doping because we know that the Néel ordered state is the correct ground state for the zero doping. For small doping, a Schwinger boson approach may be the more appropriate treatment since it connects naturally to the Néel phase.[33–37] Our hope is that, for intermediate doping, the schematic mean-field phase diagram shown in Fig. 1 is a useful starting point.

Restricting ourselves to region IV, we decouple the Hamiltonian (2.5) by a Hubbard-Stratonovitch transformation. The presence of two quartic terms can be dealt with by introducing two decoupling fields η_{ij} and χ_{ij} as follows. We insert the identity

$$\begin{aligned}1&=\int d\chi_{ij}d\chi_{ij}^{*}\delta(\chi_{ij}-f_{i\alpha}^{*}f_{j\alpha})\\&=\int d\eta_{ij}d\bar{\eta}_{ij}d\chi_{ij}d\chi_{ij}^{*}\\&\quad\times e^{\eta_{ij}(\chi_{ij}^{*}-f_{j\alpha}^{*}f_{i\alpha})+\bar{\eta}_{ij}(\chi_{ij}-f_{i\alpha}^{*}f_{j\alpha})}\end{aligned}\tag{2.8}$$

in Eq. (2.5), where the η_{ij} and $\bar{\eta}_{ij}$ are understood to be independent integration variables taken along the imaginary axis in their respective complex planes. To obtain the saddle point, each integration contour is distorted in the complex plane. We then obtain

$$\begin{aligned}Z=\int d\lambda_i d\chi_{ij}d\chi_{ij}^{*}d\eta_{ij}d\bar{\eta}_{ij}db_i db_i^{*}df_{i\sigma}df_{i\sigma}^{*}\\\times\exp\left[-\int d\tau\mathcal{L}\right],\end{aligned}\tag{2.9}$$

where

$$\begin{aligned}\mathcal{L}=\mathcal{L}_0-\frac{J}{2}\chi_{ij}f_{j\sigma}^{*}f_{i\sigma}-t\chi_{ij}b_i b_j^{*}+\text{c.c.}\\+\eta_{ij}(\chi_{ij}^{*}-f_{j\sigma}^{*}f_{i\sigma})+\bar{\eta}_{ij}(\chi_{ij}-f_{i\sigma}^{*}f_{j\sigma})\,.\end{aligned}\tag{2.10}$$

By a change of variables $(J/2)\tilde{\eta}_{ij}=\eta_{ij}+(J/2)\chi_{ij}$ and $(J/2)\tilde{\bar{\eta}}_{ij}=\bar{\eta}_{ij}+(J/2)\chi_{ij}^{*}$, Eq. (2.10) can be rewritten as

$$\begin{aligned}\mathcal{L}=\mathcal{L}_0-\frac{J}{2}\tilde{\eta}_{ij}f_{i\sigma}^{*}f_{j\sigma}-t\chi_{ij}b_i b_j^{*}+\text{c.c.}\\+\frac{J}{2}(\bar{\eta}_{ij}\chi_{ij}^{*}+\tilde{\bar{\eta}}_{ij}\chi_{ij})-J|\chi_{ij}|^2)\,.\end{aligned}\tag{2.11}$$

From the second and third terms of this equation we see that $(J/2)\tilde{\eta}_{ij}$ and $t\chi_{ij}$ play the roles of hopping integrals for the fermion and boson fields, respectively. Equation (2.11) is now quadratic in the fields f and b. The mean-field solution consists of performing the f and b integrals in Eq. (2.9) and looking for a saddle point in the variables χ_{ij}, $\bar{\eta}_{ij}$, and λ_i. Generally, the saddle point is given by $\lambda_i=i\lambda_0$ and distinguished by different symmetries of χ_{ij} and $\bar{\eta}_{ij}$. The uniform phase is the simplest case when $\chi_{ij}=\chi_0$ and $\bar{\eta}_{ij}=\tilde{\bar{\eta}}_{ij}=\eta_0$ for all nearest-neighbor bonds.[15] The π-flux phase is one where $|\chi_{ij}|$ is constant but the sum of the phase of χ_{ij} around a plaquette is π.[10] The dimerized phase is one where only one bond per site is nonzero. At half-filling, it was found that the dimerized phase is most stable.[26] The π-flux phase may be stabilized by introducing more complicated interactions but the uniform phase is unstable.[38,39] When doping is introduced it has been argued that the commensurate flux phase is the state that connects naturally to the π-flux phase.[18,19] This state breaks T and P symmetry and is related to anyon superconductivity.[21–23] For sufficiently large doping, $x\geq J/t$, Grilli and Kotliar[15] have shown in a large-N treatment that the uniform phase becomes stable. In this paper we shall restrict out attention to the uniform phase and consider fluctuations about this saddle point.

It is clear that fluctuations in the amplitude of χ_{ij} and $\tilde{\eta}_{ij}$ will acquire an energy gap of order J and can be ignored. This leaves the fluctuation in the λ field, which we write as $\lambda_i=i\lambda_0+a_0(\mathbf{r}_i)$ and the phase of χ_{ij} and $\tilde{\eta}_{ij}$. From Eq. (2.11) we see that the term $\tilde{\eta}_{ij}\chi_{ij}^{*}$ will lock the phases of $\tilde{\eta}_{ij}$ and χ_{ij} so that the out-of-phase mode will again acquire an energy gap. This leaves the in-phase degree of freedom, which we denote by θ_{ij}, as the only remaining soft mode.

With this approximation the total Lagrangian is written as $\mathcal{L}=\mathcal{L}_{\text{MF}}+\tilde{\mathcal{L}}$, where the mean-field part $\mathcal{L}_{\text{MF}}$ is the saddle-point value and the part which includes the phase fluctuation $\tilde{\mathcal{L}}$ is given by

$$\begin{aligned}\tilde{\mathcal{L}}=&\sum_{i,\sigma}f_{i\sigma}^{*}\left[\frac{\partial}{\partial\tau}-\mu_F+ia_0(\mathbf{r}_i)\right]f_{i\sigma}\\&+\sum_i b_i^{*}\left[\frac{\partial}{\partial\tau}-\mu_B+ia_0(\mathbf{r}_i)\right]b_i\\&-\frac{J}{2}\eta_0\sum_{\langle ij\rangle,\sigma}e^{i\theta_{ij}}f_{i\sigma}^{*}f_{j\sigma}-t\chi_0\sum_{\langle ij\rangle}e^{i\theta_{ij}}b_i^{*}b_j\end{aligned}\tag{2.12}$$

and the functional integral is over the variables $a_0(\mathbf{r}_i)$, θ_{ij}, b_i, b_i^{*} and f_i, f_i^{*}. The chemical potentials μ_F and μ_B are chosen to satisfy the conditions $(1/N)\sum_i b_i^{*}b_i=x$ and $(1/N)\sum_{i\sigma}f_{i\sigma}^{*}f_{i,\sigma}=1-x$, where N is the number of sites.

It is worth pointing out that Eq. (2.12) can be obtained in a simpler way[25] by rewriting Eq. (2.5) as

$$H=-\frac{J}{2}\left|f_{i\sigma}^{\dagger}f_{j\sigma}+2\frac{t}{J}b_i^{\dagger}b_j\right|2+\frac{4t^2}{J}|b_i^{\dagger}b_j|^2\tag{2.13}$$

and decoupling the first term by a standard Hubbard-Stratonovitch transformation using a single complex field χ_{ij}. The price one pays is that a four-boson term (the second term) in Eq. (2.13) is left in the Lagrangian which one has to argue away as being unimportant for small x. The resulting effective Lagrangian is then the same as Eq. (2.12) except that η_0 is replaced by χ_0.

We note that Eq. (2.12) is invariant under the local gauge transformation $f_{i\sigma}\rightarrow f_{i\sigma}e^{i\phi_i(\tau)}$, $b_i\rightarrow b_i e^{i\phi_i(\tau)}$,

$a_0(\mathbf{r}_i)\rightarrow a_0(\mathbf{r}_i)-(\partial/\partial\tau)\phi_i$, and $\theta_{ij}\rightarrow\theta_{ij}-\phi_i+\phi_j$. This is because the original problem is written in terms of the electron operator $c_{i\sigma}$, which is clearly invariant under this gauge transformation. Thus, we should write $\theta_{ij}=\tilde{\theta}_{ij}-\phi_i+\phi_j$ and the functional integral can be separated into an integration over ϕ_i and $\tilde{\theta}_{ij}$. Integration over $\tilde{\theta}_{ij}$ alone corresponds to a fixing of the gauge. This point was discussed by Ioffe and Larkin.[26] We also note that the variable $a_0(\mathbf{r}_i)$, which was initially τ independent, acquires τ dependence under the gauge transformation. Equation (2.12) describes fermions and bosons hopping on a square lattice with complex hopping matrix elements and subject to a scalar potential $a_0(\mathbf{r}_i)$. We note that the Lagrangian of particles hopping in the presence of a magnetic field perpendicular to the plane is also described by complex hopping matrix elements such that the sum of the phases around a plaquette $\theta_{\rm tot}=\theta_{12}+\theta_{23}+\theta_{34}+\theta_{41}$ equals the magnetic flux through the plaquette. $\theta_{\rm tot}$ is, of course, invariant under gauge transformations. We then introduce the gauge field variables a_x and a_y defined in the middle of the bonds such that

$$\tilde{\theta}_{ij}=(\mathbf{r}_j-\mathbf{r}_j)\cdot\mathbf{a}[(\mathbf{r}_i+\mathbf{r}_j)/2] .$$

In the continuum limit this defines gauge fields $a_x(\mathbf{r},\tau)$ and $a_y(\mathbf{r},\tau)$ such that the line integral $\oint\mathbf{a}\cdot d\mathbf{l}$ around a plaquette reproduces $\theta_{\rm tot}$. Defining the two-dimensional curl of $\mathbf{a}$,

$$h=\nabla\times\mathbf{a}\equiv\epsilon_{jk}\frac{\partial}{\partial x_j}a_k , \tag{2.14}$$

we have

$$hc_0^2=\theta_{\rm tot} , \tag{2.15}$$

where c_0 is the lattice constant. Thus, Eq. (2.12) has the natural interpretation of fermions and bosons subject to a set of gauge fields (a_0,a_x,a_y) that fluctuates in space and time.

If $x\ll 1$, the number of bosons is small and only long-wavelength boson excitations are important. In this case the tight-binding model can be approximated by a continuum model with an effective mass m_B where $c_0^{-2}/m_B=2t$. For fermions only excitations near the Fermi sea are expected to be important. For simplicity it is also convenient to approximate the fermion tight-binding band by an isotropic band with mass m_F where $c_0^{-2}m_F^{-1}=2J$. For most purposes in this paper, only the density of states at the Fermi level is important and the isotropic band approximation does not change the essential physics. However, very close to half-filling ($x\ll 1$) the Fermi surface is nearly a square and nesting properties are important for consideration of the spin-spin correlation function. Under these simplifications, we arrive at the following continuum Lagrangian:

$$\begin{aligned}\mathcal{L}=\int d^2\mathbf{r}\Bigg[&\sum_\sigma f_\sigma^*(r)\left(\frac{\partial}{\partial\tau}-\mu_F+ia_0\right)f_\sigma(r)\\&+b^*(r)\left(\frac{\partial}{\partial\tau}-\mu_B+ia_0\right)b(r)\\&-\frac{1}{2m_F}\sum_{\sigma,j=x,y}f_\sigma^*\left(\frac{\partial}{\partial x_j}+ia_j\right)^2 f_\sigma\\&-\frac{1}{2m_B}\sum_{j=x,y}b^*\left(\frac{\partial}{\partial x_j}+ia_j\right)^2 b\Bigg] .\end{aligned} \tag{2.16}$$

The bulk of this paper consists of analysis of this effective Lagrangian. We note that Eq. (2.16) can be written down phenomenologically as the simplest Lagrangian involving fermions and bosons which respect the local gauge symmetry $f\rightarrow fe^{i\theta}$, $b\rightarrow be^{i\theta}$, and $\mathbf{a}\rightarrow\mathbf{a}+\nabla\theta$. It is important to note that Eqs. (2.12) and (2.16) describe systems which satisfy the *local* constraint (2.3) exactly. This is clearly demonstrated[32] by introducing the variable.

$$Q_i=\sum_\sigma f_{i\sigma}^\dagger f_{i\sigma}+b_i^\dagger b_i \tag{2.17}$$

and adding a term $i\tilde{A}_0Q_i$ to $\mathcal{L}$. All correlation functions of Q_i can be generated by taking the functional derivative of $\ln Z$ with respect to $\tilde{A}_0$. It is clear that $\tilde{A}_0$ appears in Z as a shift of a_0 to $a_0+\tilde{A}$. By a change of variable of integration, it is obvious that, upon performing the a_0 integration, Z is independent of $\tilde{A}_0$, so that all correlation functions involving Q_i vanish and $Q_i-1=0$ can be considered an operator identity. Similarly, we can consider

$$\mathbf{J}_i=\mathbf{J}_{iF}+\mathbf{J}_{iB} , \tag{2.18}$$

which is the sum of the fermion and boson current on each bond in the lattice problem and everywhere in space in the continuum theory. By introducing a term $\tilde{A}_i$ to the Lagrangian, we see that the spatial component of the gauge field $\mathbf{a}_i$ is shifted by $\mathbf{a}_i+\tilde{A}_i$ so that, upon integration, Z is independent of $\tilde{A}_i$ and $\mathbf{J}_i=0$ as an operator identity. Thus, the role of the spatial component of the gauge field is to enforce the constraint that the sum of the fermion and boson current on each bond must be identically zero because a fermion hopping to the right is necessarily accompanied by a boson hopping to the left. This requirement lies at the heart of the Ioffe-Larkin composition rules which relate physical response functions to fermion and boson response functions as we shall discuss later.

III. PHYSICAL MEANING OF THE GAUGE FIELD

Up to now the gauge field $\mathbf{a}$ has been introduced as the phase of χ_{ij} and appears to be an abstract mathematical entity. The field $\mathbf{a}$ itself is not gauge invariant and has no direct physical content, but the "magnetic flux" h associated with $\mathbf{a}$ defined by

$$\begin{aligned}h&=\nabla\times\mathbf{a}\\&\equiv\frac{\partial a_y}{\partial x}-\frac{\partial a_x}{\partial y}\end{aligned} \tag{3.1}$$

is gauge invariant and turns out to have a very direct physical meaning in terms of observable quantities. This connection was first made explicitly by Wen, Wilczek, and Zee[20] in the case of the quantum spin model at half-filling. We shall extend their discussion to the t-J model away from half-filling. Let us first consider four sites around a plaquette labeled by 1,2,3,4 in an anticlockwise manner as shown in Fig. 2(a), and define

$$P_{1234}=\langle \chi_{12}\chi_{23}\chi_{34}\chi_{41}\rangle \ . \tag{3.2}$$

From Eq. (2.9), χ_{ij} is conjugate to the operator $f^\dagger_{i\sigma} f_{j\sigma}$, so that

$$P_{1234}=\langle f^\dagger_{1\alpha} f_{2\alpha} f^\dagger_{2\beta} f_{3\beta} f^\dagger_{3\gamma} f_{4\gamma} f^\dagger_{4\delta} f_{1\delta}\rangle \ . \tag{3.3}$$

In fact, let us consider the simpler case of three sites forming a triangle

$$P_{123}\equiv\langle f^\dagger_{1\alpha} f_{2\alpha} f^\dagger_{2\beta} f_{3\beta} f^\dagger_{3\gamma} f_{1\gamma}\rangle \tag{3.4}$$

and relate this to physical observables. For this purpose the following identities are very useful:

$$f^\dagger_{i\alpha} f_{i\beta}=\tfrac{1}{2}\tilde{\rho}_i\delta_{\alpha\beta}+\mathbf{S}_i\cdot\boldsymbol{\sigma}_{\alpha\beta} \ , \tag{3.5a}$$

$$f_{i\alpha} f^\dagger_{i\beta}=\tfrac{1}{2}(2-\tilde{\rho}_i)\delta_{\alpha\beta}-\mathbf{S}_i\cdot\boldsymbol{\sigma}_{\alpha\beta} \ , \tag{3.5b}$$

where $\tilde{\rho}_i\equiv\sum_\alpha f^\dagger_{i\alpha} f_{i\alpha}$, $\mathbf{S}_i=\frac{1}{2} f^\dagger_{i\alpha}\boldsymbol{\sigma}_{\alpha\beta} f_{i\beta}$ are the fermion density and the spin operator on site i and $\boldsymbol{\sigma}_{\alpha\beta}$ are the Pauli matrices. At half-filling, $\tilde{\rho}=1$. It is worth pointing out that, away from half-filling, the electron spin operator is still given by $f^\dagger_\alpha\boldsymbol{\sigma}_{\alpha\beta} f_\beta$, even though the electron operator is represented as $c_\alpha=f_\alpha b^\dagger$ and the electron density is not $\tilde{\rho}$. This is because $f^\dagger_\alpha\boldsymbol{\sigma}_{\alpha\beta} f_\beta$ has the same matrix elements in the constrained subspace as the spin operator. For example, we can write

$$S^\dagger_i=f^\dagger_{i\downarrow} f_{i\downarrow} b_i b^\dagger_i=f^\dagger_{i\uparrow} f_{i\downarrow}(f^\dagger_{i\uparrow} f_{i\uparrow}+f^\dagger_{i\downarrow} f_{i\downarrow}) \ ,$$

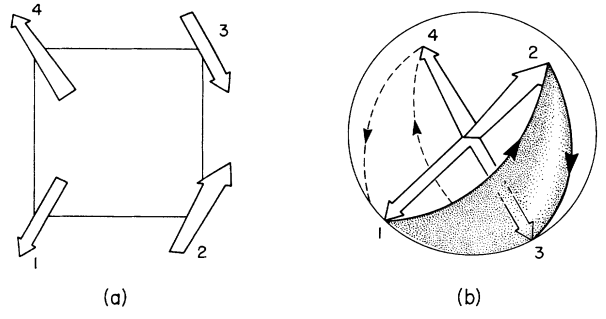

FIG. 2. (a) Four sites around a square plaquette with an instantaneous spin configuration. The spin on site 2 points out of the plane while the spin on site 4 points into the plane. (b) The tip of the unit vectors representing the instantaneous spin orientation shown in (a) are put on the surface of a sphere. In this example, spin 2 is on the front hemisphere while spin 4 is on the rear hemisphere. The path 1234 traces out a solid angle which can be interpreted as the gauge flux through the plaquette. Note that, if spins 2 and 4 both point out of the plane, the solid angles formed by 123 and 341 will have opposite sign and tend to cancel each other.

which equals $f^\dagger_{i\uparrow} f_{i\downarrow}$. It is possible to derive an operator identity, relating the operators in Eq. (3.4) to the spin operator $\mathbf{S}$ and $\tilde{\rho}$. Defining the operator $\hat{P}_{123}\equiv f^\dagger_{1\alpha} f_{2\alpha} f^\dagger_{2\beta} f_{3\beta} f^\dagger_{3\gamma} f_{1\gamma}$, we commute $f^\dagger_{1\alpha}$ to be next to $f_{1\gamma}$ and use Eqs. (3.5a) and (3.5b):

$$\hat{P}_{123}=\mathrm{Tr}\{[\tfrac{1}{2}(2-\tilde{\rho}_2)I-\mathbf{S}_2\cdot\boldsymbol{\sigma}][\tfrac{1}{2}(2-\tilde{\rho}_3)I-\mathbf{S}_3\cdot\boldsymbol{\sigma}] \times(\tfrac{1}{2}\tilde{\rho}_1 I+\mathbf{S}_1\cdot\boldsymbol{\sigma})\} \ , \tag{3.6}$$

where I is the identity matrix and the trace is over spin indices. The trace can be done using the identities $\mathrm{Tr}(\sigma_i\sigma_j)=2\delta_{ij}$, $\mathrm{Tr}(\sigma_i\sigma_j\sigma_k)=2i\epsilon_{ijk}$, and we obtain

$$\hat{P}_{123}=\tfrac{1}{4}(2-\tilde{\rho}_2)(2-\tilde{\rho}_3)\tilde{\rho}_1-(2-\tilde{\rho}_2)\mathbf{S}_3\cdot\mathbf{S}_1 -(2-\tilde{\rho}_3)\mathbf{S}_2\cdot\mathbf{S}_1+\tilde{\rho}_1\mathbf{S}_2\cdot\mathbf{S}_3+2i\mathbf{S}_2\cdot(\mathbf{S}_3\times\mathbf{S}_1) \ . \tag{3.7}$$

As pointed out by Wen, Wilczek, and Zee, the quantity of interest is $\hat{P}_{123}-\hat{P}_{132}$, i.e., the difference between going around the triangle in the counterclockwise and clockwise directions. Only the last term in Eq. (3.7) survives, which can be written as $\hat{P}_{123}-\hat{P}_{132}=4i\hat{E}_{123}$, where $\hat{E}_{123}$ is the spin chirality operator defined as

$$\hat{E}_{123}=\mathbf{S}_1\cdot(\mathbf{S}_2\times\mathbf{S}_3) \ . \tag{3.8}$$

It is an operator which breaks parity and time-reversal symmetry and plays an important role in the chiral spin liquid theory where $\hat{E}_{123}$ acquires a nonvanishing expectation value in the ground state. In the uniform RVB state we are considering, $\langle\hat{E}_{123}\rangle=0$ and we will be interested in the fluctuations in the chirality and correlation functions of the chirality operators. This is why it is important for us to establish the relation between $\hat{P}_{123}$ and $\hat{E}_{123}$ as operator identities.

The above discussion can readily be extended to the four-site case. Defining

$$\hat{P}_{1234}=f^\dagger_{1\alpha} f_{2\alpha} f^\dagger_{2\beta} f_{3\beta} f^\dagger_{3\gamma} f_{4\gamma} f^\dagger_{4\delta} f_{1\delta} \ ,$$

we can show that

$$\hat{P}_{1234}-\hat{P}_{1432}=2i\{(2-\tilde{\rho}_2)\hat{E}_{134}+(2-\tilde{\rho}_4)\hat{E}_{123} +(2-\tilde{\rho}_3)\hat{E}_{124}-\tilde{\rho}_1\hat{E}_{234}\} \ . \tag{3.9}$$

For half-filling, $\tilde{\rho}=1$ and Eq. (3.9) reduces to the expression of Wen, Wilczeck, and Zee. In that case, the first two terms in Eq. (3.9) are the sum of the chirality around the two triangles formed by cutting the square with a line through site 1 whereas the last two terms are the difference of the chirality around the triangles with a different orientation. Note that site 1 is the starting point of the "hop" around the square and plays a special role. To obtain a more symmetrical expression, we can define an average over the starting point so that

$$\begin{aligned}\hat{E}_{1234}&=\frac{-i}{4}\{\hat{P}_{1234}+\hat{P}_{2341}+\hat{P}_{3412} +\hat{P}_{4123}-\text{clockwise terms}\}\\ &=\{(3-2\tilde{\rho}_2)\hat{E}_{134}+(3-2\tilde{\rho}_4)\hat{E}_{123} +(3-2\tilde{\rho}_3)\hat{E}_{124}+(3-2\tilde{\rho}_1)\hat{E}_{234}\} \ .\end{aligned} \tag{3.10}$$

This expression may reasonably be interpreted as the chirality operator for a square plaquette.

Now we want to relate $\hat{E}_{1234}$ to the gauge field. Starting from Eq. (3.2) and ignoring amplitude fluctuations, we have

$$\langle \hat{P}_{1234}-\hat{P}_{1432}\rangle=\chi_0^4\langle e^{i(\theta_{12}+\theta_{23}-\theta_{43}-\theta_{14})}-\text{c.c.}\rangle \ . \tag{3.11}$$

The combination of θ_{ij} in the exponent is the sum of the gauge field variables around a plaquette which is the gauge-invariant flux Φ through the plaquette and which becomes the magnetic flux h defined in Eq. (3.1) in the continuum limit. Comparing Eqs. (3.10) and (3.11), we see that $\langle \sin\Phi\rangle$ is proportional to the average chirality $\langle \hat{E}_{1234}\rangle$. Of course, for the ground state we are considering, this quantity is zero. However, this argument can be extended to any correlation function of $\sin\Phi$ and of the chirality. Thus, we conclude that correlation functions involving $\sin\Phi$ can be identified with correlation functions of chirality. Here the fluctuation in the gauge field can be interpreted as fluctuations in the chirality through each plaquette. However, it should be noted that this is true only for the low-frequency components. For higher frequencies, the amplitude fluctuation dominates, which is neglected in Eq. (3.11).

It is important to distinguish the gauge field discussed in this paper from the staggered gauge field which has been introduced in the literature.[40–43] The staggered gauge field typically arises in the Schwinger-boson–slave-fermion version of the theory, where two sublattices are introduced. The spin quantization axis is reversed on opposite sublattices and a slowly varying sublattice magnetization variable $\hat{\Omega}$ is introduced. The staggered gauge field corresponds to the local gauge transformation where $b_j\rightarrow b_j e^{\pm i\phi}$, where $\pm$ depends on the sublattices the site j belongs to. The corresponding staggered flux $\mathbf{h}_s=\nabla\times\mathbf{a}_s$ is then related to the staggered chirality. On a lattice, the staggered chirality would look like Eq. (3.10) but with the spin reversed on sites 1 and 3. At half-filling we have

$$\hat{E}_{1234,\text{staggered}}=\hat{E}_{123}+\hat{E}_{134}-\hat{E}_{124}-\hat{E}_{234} \ . \tag{3.12}$$

This can also be written as $(\mathbf{S}_1-\mathbf{S}_2)\cdot[(\mathbf{S}_2-\mathbf{S}_3)\times(\mathbf{S}_3-\mathbf{S}_4)]$, which in the continuum limit becomes $\hat{\Omega}_1\cdot(\hat{\Omega}_2\times\hat{\Omega}_3)$, the chirality corresponding to the staggered magnetization. The purpose of this discussion is to emphasize that the staggered flux or staggered chirality is an object quite independent of the uniform flux or uniform chirality and should not be confused with the uniform chirality fluctuation evaluated at a staggered wave vector (π,π) as is sometimes done in the literature.[44]

In the case of the staggered gauge field, there is an another interpretation of the staggered flux h_s which has a more transparent geometrical meaning. The instantaneous flux is given by the phase $\Phi_w=\frac{1}{2}W(\hat{\Omega}_1,\hat{\Omega}_2,\hat{\Omega}_3)$, where W is the solid angle subtended by the instantaneous sublattice magnetization $\hat{\Omega}_i$ on the three sites when the tips of the unit vectors are placed on the surface of a sphere.[42,43] A similar interpretation can be given to the uniform gauge field. However, in this case the spin $\mathbf{S}_i$ are not in the same general direction and the solid angle between them can be large, so that the geometrical picture is not as clear as in the staggered case. Nevertheless, for completeness we outline the relationship here. In order to relate the flux to the instantaneous spin orientation, we need to introduce the coherent state representation of an $S=\frac{1}{2}$ spin. The most natural definition is to consider the spin direction $\hat{\mathbf{n}}$ as specifying a quantization axis so that the state $|\hat{\mathbf{n}}\rangle$ means that a fermion is occupied with spin up along the quantization axis $\hat{\mathbf{n}}$. This is accomplished by introducing the rotation matrix in spin space $D_{\alpha\beta}(\hat{\mathbf{n}})$ and defining $f'_\alpha\equiv D_{\alpha\beta}(\hat{\mathbf{n}})f_\beta$. Now we can prove the following statement. The operator $\hat{P}_{123}$, when evaluated between the coherent state $|\hat{\mathbf{n}}_1\hat{\mathbf{n}}_2\hat{\mathbf{n}}_3\rangle\equiv|\hat{\mathbf{n}}_1\rangle|\otimes\hat{\mathbf{n}}_2\rangle\otimes|\hat{\mathbf{n}}_3\rangle$, has the value

$$\langle \hat{\mathbf{n}}_1\hat{\mathbf{n}}_2\hat{\mathbf{n}}_3|\hat{P}_{123}-\hat{P}_{132}|\hat{\mathbf{n}}_1\hat{\mathbf{n}}_2\hat{\mathbf{n}}_3\rangle=\left[\frac{1+\hat{\mathbf{n}}_1\cdot\hat{\mathbf{n}}_2}{2}\right]^{1/2}\left[\frac{1+\hat{\mathbf{n}}_2\cdot\hat{\mathbf{n}}_3}{2}\right]^{1/2}\left[\frac{1+\hat{\mathbf{n}}_3\cdot\hat{\mathbf{n}}_1}{2}\right]^{1/2}\exp\left[\frac{i}{2}W(\hat{\mathbf{n}}_1,\hat{\mathbf{n}}_2,\hat{\mathbf{n}}_3)\right]-\text{c.c.} \tag{3.13}$$

This follows by first commuting $f^\dagger_{1\alpha}$ in $\hat{P}_{123}$ through to the right. The correction term $\delta_{\alpha\gamma}f_{2\alpha}f^\dagger_{2\beta}f_{3\beta}f^\dagger_{3\gamma}$ can easily be shown to give rise to a real constant which cancels in Eq. (3.13). Next we express f in terms of f' and, upon computing the matrix element, it is obvious that all the spin labels on f'_α are spin $\downarrow$. We then obtain

$$\langle\uparrow\uparrow\uparrow|\hat{P}_{123}|\uparrow\uparrow\uparrow\rangle=-M(\hat{\mathbf{n}}_1,\hat{\mathbf{n}}_3)M(\hat{\mathbf{n}}_3,\hat{\mathbf{n}}_2)M(\hat{\mathbf{n}}_2,\hat{\mathbf{n}}_1)+\text{const} \ ,$$

where

$$M(\hat{\mathbf{n}}_2,\hat{\mathbf{n}}_1)\equiv[D(\hat{\mathbf{n}}_2)^\dagger D(\hat{\mathbf{n}}_1)]_{\downarrow\downarrow}=e^{-i(1/2)W(\hat{\mathbf{n}}_1,\hat{\mathbf{n}}_2,\hat{\mathbf{n}}_3)}(1+\hat{\mathbf{n}}_1\cdot\hat{\mathbf{n}}_2)^{1/2}$$

from which Eq. (3.13) follows. This discussion can be extended to $\hat{P}_{1234}-\hat{P}_{1432}$, and by comparison with Eq. (3.11) we are led to the identification of the gauge flux through the plaquette with the solid angle traced out by the instantaneous spin orientations. An example is shown in Fig. 2(b). However, this geometrical picture breaks down if any two spins are nearly antiparallel, in which case the amplitude term $(1+\hat{\mathbf{n}}_1\cdot\hat{\mathbf{n}}_2)^{1/2}$ nearly vanishes and the solid angle undergoes large fluctuations. The chirality remains small even in this case and is probably a more useful concept.

IV. GAUGE FIELD PROPAGATOR AND THE REIZER SINGULARITY

In the remainder of this paper, we will explore the physical consequence of the effective Lagrangian, Eq.

(2.16). In earlier discussion of this model,[15] the bosons are assumed to bose condense so that $\langle b \rangle = b_0$. In this case, the electron operator $c_\sigma^\dagger = b f_\sigma^\dagger \approx b_0 f_\sigma^\dagger$ and we end up with a Fermi-liquid theory very similar to that developed for the heavy-fermion problem. In this paper we work at a finite temperature and assume that the bosons are not Bose condensed. It turns out that the gauge field fluctuations are now centered at low momentum and energy, leading to interesting new physics.

We begin by performing perturbation theory in the coupling between the fermions or bosons with the gauge field. In order to do this, we first obtain an expression for the gauge field propagator $D_{\mu\nu}(\mathbf{r},\tau) = \langle T_\tau a_\mu(\mathbf{r},\tau) a_\nu^\dagger(0) \rangle$ by integrating out quadratic fermion and boson fluctuations. The time and space components (labeled i,j) of the gauge field decouple and we shall concentrate on the spatial components only, since the time component is screened by density fluctuations and will give rise to only a short-range force. The spatial part D_{ij} is given by $D_{ij} = (\Pi_F^{JJ} + \Pi_B^{JJ})_{ij}^{-1}$, where

$$\Pi_{F,ij}^{JJ}(\mathbf{r},\tau) = -\langle T_r [J_{F_i}(\mathbf{r},\tau) J_{F_j}(0,0) - \delta_{ij}\rho_F \delta(\mathbf{r})\delta(\tau)] \rangle \tag{4.1}$$

and similarly for Π_B^{JJ}. Here $\mathbf{J}_F = i f^\dagger (\nabla/2m_F) f + \text{c.c.}$ is the fermion current operator and $\rho_F = f^\dagger f$. It is convenient to choose the Coulomb gauge $\nabla \cdot \mathbf{a} = 0$, in which case the spatial part of the gauge field is purely transverse. In Fourier space, we have

$$D_{ij}(\mathbf{q},\omega) = (\delta_{ij} - q_i q_j / q^2) D^T(\mathbf{q},\omega) , \tag{4.2}$$

where the retarded propagator

$$D^T(\mathbf{q},\omega) = [\Pi_F^T(\mathbf{q},\omega) + \Pi_B^T(\mathbf{q},\omega)]^{-1}$$

is the inverse of the sum of the fermion and boson polarization. For example, $\Pi^T(\mathbf{q},\omega) = i\omega\sigma^T(\mathbf{q},\omega)$, where σ^T is the transverse conductivity. In a normal Fermi liquid, the current-current correlation response function [first term in Eq. (4.1)] cancels the diamagnetic term [second term in Eq. (4.1)] in the $\mathbf{q},\omega \to 0$ limit and we can write, for $v_F q \ll \epsilon_F$,

$$\Pi_F^T(\mathbf{q},\omega) = i\omega\sigma_{F1}^T(\mathbf{q},\omega) - \chi_F q^2 , \tag{4.3}$$

where χ_F is the Landau diamagnetic susceptibility of the Fermi system which equals $1/(24\pi m_F)$ for a free fermion in two dimensions (2D). That this identification is reasonable can be seen from the definition $\chi_F = \partial M^T/\partial h$, $\nabla \times M^T = \mathbf{J}_F$, and $\nabla \times \mathbf{a} = \mathbf{h}$. Thus, in Fourier space $\Pi_F^T = \partial \langle \mathbf{J}_F \rangle / \partial \mathbf{a} = q^2 \chi_F$ is the appropriate $\omega \to 0$ limit in Eq. (4.3). The first term in Eq. (4.3) describes the dissipation and $\sigma_{F1}^T(\mathbf{q},\omega)$ is the real part of the conductivity. It is convenient to introduce an inverse lifetime γ_q by parametrizing $\sigma_{F1}^T(\mathbf{q},\omega) = \rho_F/(m_F\gamma_q)$ as the static limit of the conductivity which is valid when $\omega < \gamma_q$. We have

$$\gamma_q = \begin{cases} \tau_{\text{tr}}^{-1} & \text{for } q < (v_F\tau_{\text{tr}})^{-1} \quad (4.4a) \\ v_F q/2 & \text{for } q > (v_F\tau_{\text{tr}})^{-1} , \quad (4.4b) \end{cases}$$

where τ_{tr} is the transport time due to scattering mechanisms such as disorder or inelastic scattering at finite temperatures. Equation (4.4b) describes the familiar Landau damping so that $\sigma_{F1}^T \to 2\rho_F/(m_F v_F q)$ in this limit.[45]

A similar expression is obtained for

$$\Pi_B^T(\mathbf{q},\omega) = |i\omega| \sigma_{B1}^T(\mathbf{q},\omega_n) - \chi_B q^2 , \tag{4.5}$$

where

$$\chi_B = \frac{n(0)}{48\pi m_B} , \tag{4.6}$$

where $n(\epsilon)$ is the Bose occupation factor. We note that $n(0) = T_{BE}^{(0)}/T$ for $T \gg T_{BE}^{(0)}$, where $T_{bE}^{(0)} = 2\pi x/m_B$ is the mean-field Bose condensation temperature and that χ_B diverges for $T \ll T_{BE}^{(0)}$. In 2D, the free Bose gas does not Bose condense at any finite temperature. However, with any repulsive interaction a superfluid transition occurs below which $\chi_B q^2$ should be replaced by ρ_s/m, where ρ_s is the superfluid density. This is because the two terms in Eq. (4.1) no longer cancel each other due to the Anderson-Higgs mechanism. Thus, the form Eq. (4.5) is valid only above the superfluid transition, which, as mentioned earlier, corresponds to the onset of a Fermi-liquid phase in the present problem. In the remainder of this paper we shall restrict our attention to the high-temperature phase where Eq. (4.5) is valid. In this regime, the boson conductivity is given by

$$\sigma_{B1}^T \approx x^{1/2}/q \tag{4.7}$$

for $q > l_B^{-1}$, where l_B is the mean free path due to scattering mechanisms. Comparing Eqs. (4.7) and (4.4b) shows that $\sigma_{B1}^T \ll \sigma_{F1}^T$ and we should ignore its contribution from here on. We also introduce the parameter $\chi_d = \chi_F + \chi_B$ (we emphasize that χ_d is not the physical diamagnetic susceptibility $\tilde{\chi}$ of the system, the latter being given by $\tilde{\chi}^{-1} = \chi_F^{-1} + \chi_B^{-1}$ as shown later). In the regime $T > T_{BE}^{(0)}$, we shall adopt the following form for the retarded transverse gauge field propagator:

$$D^T(q,\omega) = [i\omega\sigma(q) - \chi_d q^2]^{-1} , \tag{4.8}$$

where

$$\sigma(q) \approx \begin{cases} k_0/q & \text{for } ql > 1 \quad (4.9a) \\ k_0 l & \text{for } ql < 1 , \quad (4.9b) \end{cases}$$

where l is the Fermion mean free path and k_0 is of order k_F which for small doping is of order the inverse of the lattice spacing. This is the form that we shall use in the remainder of the paper. We also note that, for $T > T_{BE}^{(0)}$, χ_d is dominated by χ_F which is temperature independent. The restriction to $T > T_{BE}^{(0)}$ is the most serious drawback of this work because, if we assume that the boson mass corresponds to a hopping matrix element equal to J, we have [see Eq. (6.2) for a more detailed discussion]

$$T_{BE}^{(0)} = 4\pi x J , \tag{4.10}$$

which is a temperature of order 1000 K. For our theory to apply to any reasonable temperature, we need a mechanism to suppress the onset of superfluidity (i.e., suppress

the growth of χ_B as temperature is decreased). We shall later argue that the inelastic scattering of the bosons by gauge field fluctuations provide just such a mechanism. For the time being we shall proceed to explore the physical consequence of Eq. (4.8).

The gauge field propagator Eq. (4.8) turns out to be similar in form to the transverse photon propagator in a metal. The difference in that case is that the photon has its own dynamics and a term $(1/8\pi)F_{\mu\nu}^2/e^2$ is added to the Lagrangian such as Eq. (2.16). The photon is coupled to current fluctuations in the metal and in three dimensions the propagator is

$$P^T(q,\omega)=-[-\omega^2+c^2q^2-i\omega\sigma(q)+\chi_d q^2]^{-1}\ , \tag{4.11}$$

where in our notation χ_d of a 3D free-electron gas is $\chi_d=e^2k_F/12\pi^2m$. For $\omega\ll\epsilon_F$ the ω^2 term can be ignored and $\chi_d/c^2\approx r_s(v_F/c)^2$ is the standard Landau diamagnetism which is much less than unity. Thus, we have the same functional form as Eq. (4.8) except that χ_d is replaced by c^2. The important point is that the spectral weight of excitations of gauge fluctuations for pure metals of the form

$$\mathrm{Im}P^T(q,\omega)=\frac{\omega q}{\omega^2+Cq^6}\ , \tag{4.12}$$

if we use $\sigma(q)\sim q^{-1}$, has a divergent weight for small q and ω. That coupling to these low-frequency fluctuations would lead to deviation from Fermi-liquid theory was already recognized by Holstein, Norton, and Pincus[46] in 1973, who showed that the specific heat is proportional to $(v_F/c)^2T\ln T$ instead of the standard γT term. These effects were rediscovered by Reizer,[47] who found singular corrections to density of states and conductivity due to scattering by transverse photons. Mathematically this phenomenon is quite similar to the interaction correction effects in disordered metals discovered by Altshuler and Aronov,[48] in which case the diffusion pole gives to low-lying spectral weight of the form $\mathrm{Im}(i\omega+Dq^2)^{-1}$, where D is the diffusion constant. It is worth noting that, for transverse photons, Eq. (4.12) is limited to 3D because, even if the metal is two dimensional, the electromagnetic field is generally 3D, unless special effort is made to confine the electromagnetic field to a thin layer. Thus, the gauge field in the strongly correlated metal offers a unique opportunity to explore the consequence of these low-lying excitations in 2D because, in our case, the gauge field is confined to the plane. Secondly, in the electromagnetic field case, the effect is down by the ratio $(v_F/c)^2$, whereas in the case of gauge field the coupling constant is of order unity because the speed of light does not appear in Eq. (4.8). Thus, this anomalous scattering term becomes the dominant scattering mechanism in our case.

We begin by calculating the self-energy $\Sigma(k,\Omega)$ of the fermion Green function due to scattering by the gauge field in two dimensions. The Feynman diagram is shown in Fig. 3. We focus on the imaginary part of Σ'' evaluated on the mass shell $\Omega=\epsilon_k$, which is simply the Fermi golden rule for the probability of emission of gauge field excitations

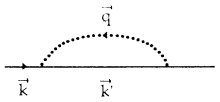

FIG. 3. Self-energy correction to the fermion or boson propagator. The dotted line represents the gauge field.

$$\begin{aligned}\Sigma''(k,\epsilon_k)=\int_0^\infty d\omega\int\frac{d\mathbf{k}'}{(2\pi)^2}&[n(\omega)+1][1-f(\epsilon_{k'})]\\&\times(\mathbf{k}+\mathbf{k}')_\alpha(\mathbf{k}+\mathbf{k}')_\beta(2m_F)^{-2}\\&\times(\delta_{\alpha\beta}-q_\alpha q_\beta/q^2)\mathrm{Im}D^T(\mathbf{q},\omega)\\&\times\delta(\epsilon_k-\epsilon_{k'}-\omega)\ ,\end{aligned} \tag{4.13}$$

where $\mathbf{q}=\mathbf{k}'-\mathbf{k}$, $n(\omega)$ and $f(\omega)$ are the boson and fermion occupation numbers, and we have used the vector coupling vertex $(\mathbf{k}+\mathbf{k}')\cdot\mathbf{a}(2m_F)^{-1}$ in Eq. (2.16). As usual, only states $\mathbf{k}'$ near the Fermi surface contribute and it is convenient to introduce the variable $\xi_k=\epsilon_k-\mu$:

$$\begin{aligned}\Sigma''(k,\epsilon_k)=\frac{-N(0)}{2\pi m_F^2}\int_0^\infty d\omega\int d\xi' d\theta&[n(\omega)+1][1-f(\xi')]\\&\times\frac{(\omega q/k_0)|\mathbf{k}\times\hat{\mathbf{q}}|^2}{\omega^2+(\chi_d q^3/k_0)^2}\\&\times\delta(\xi_k-\xi'-\omega)\ ,\end{aligned} \tag{4.14}$$

where θ is the angle between $\mathbf{k}$ and $\mathbf{k}'$ so that $q=2k_F\sin(\theta/2)$, $N(0)=m_F/2\pi$ is the density of states, and Eq. (4.8) in the clean limit Eq. (4.9a) has been used. First we evaluate Eq. (4.14) at $T=0$. It is clear that the integrand is dominated by small q, in which case

$$\Sigma''(k,\epsilon_k)=\frac{-k_FN(0)}{2\pi m_F^2}\int_0^{\xi_k}d\omega\int_0^\infty dq\frac{\omega q/k_0}{\omega^2+(\chi_d q^3/k_0)^2}\ . \tag{4.15}$$

The q integration can be done by scaling, yielding $\omega^{-1/3}\chi_d^{-2/3}k_0^{-1/3}$. The ω integration then gives the result

$$\Sigma''(k,\epsilon_F)\approx -C\xi_k^{2/3}\ ,$$

where the constant $C\approx(k_F/m_F)\chi_d^{-2/3}k_0^{-1/3}$. The important point is that an analogous calculation of Σ'' due to scattering by screened longitudinal or any other short-range interaction would have yielded the standard Fermi-liquid result proportional to ξ_k^2. The anomalously large scattering rate given by the above equation results from the abundance of small q and ω fluctuations in the transverse gauge field. We remark that, if in the disordered limit Eq. (4.9b) were used, we would have obtained $\Sigma''\sim\xi_k$, a result familiar in the interaction effect lifetime.[48]

Next we evaluate Eq. (4.14) at finite temperature T and we encounter a surprise. The ξ and θ integrations are evaluated as before and, for $\omega<T$, the bose factor $n(\omega)$ can be approximated by T/ω. Now we find

$$\Sigma'' \approx -CkT \int_0^{\xi_k} d\omega\, \omega^{-4/3} , \tag{4.16}$$

which is a divergent integral. Since the small-q and ω limits of the integrand have been treated accurately, there is no possibility of a cutoff to cure the divergence. The origin of the divergence can best be understood by considering the fermion Green function in space and time. We can use the Gorkov approximation to write

$$G(\mathbf{r},t) = G_0(r,t)\left\langle \exp\left[i \int_L \mathbf{a}\cdot d\mathbf{l} \right] \right\rangle_{\mathrm{a}} , \tag{4.17}$$

where L is a straight-line path connecting (0,0) and $(\mathbf{r},t)$ and G_0 is the Green function without gauge field. We note that $G(\mathbf{r},t)$ is not gauge invariant under the gauge transformation $f_\sigma \rightarrow f_\sigma e^{i\theta}$ and any further discussion must be done in fixed gauge. Once the gauge is fixed, we can compute $\langle \exp(i\int_L \mathbf{a}\cdot d\mathbf{l}) \rangle_{\mathrm{a}}$ by averaging over gauge field fluctuations. This is done in Appendix A where we show in two dimensions that this quantity vanishes whenever $\mathbf{r} \neq 0$. Thus, in two dimensions, the fluctuating gauge field is sufficient to make the Green function vanish everywhere except when the spatial points coincide at any finite temperature. The divergence of Σ'' is an indication of this general feature.

The vanishing of $G(\mathbf{r},t)$ need not cause as much concern as it first appears because G itself is not gauge invariant. It would typically appear in the intermediate state of a diagrammatic calculation of a gauge-invariant quantity and the divergences should cancel for any physical quantity. This is illustrated by considering the transport time instead of the self-energy. Since τ_{tr}^{-1} is the momentum relaxation rate, it is given by Eq. (4.14) with an additional q^2 factor in the integrand. The q integration now gives $\omega^{-2/3}$ leading to

$$\tau_{\mathrm{tr}}^{-1} \propto \begin{cases} \xi_k^{4/3} & \text{for } \xi_k > kT , \\ T^{4/3}, & kT > \xi_k . \end{cases} \tag{4.18}$$

As expected, the transport time which enters into the expression for fermion conductivity σ_F is now finite, even though it is still enhanced compared with the usual Fermi-liquid result.

The discussion of the boson lifetime proceeds along similar lines. The boson self-energy $\Sigma_B(k,\omega_k)$ is the same as in Eq. (4.13) except that $1-f(\epsilon_{k'})$ is replaced by $1+n(\omega_{k'})$ and ϵ_k is replaced by ω_k in the δ function, where ω_k is the boson dispersion. At finite temperature $T > T_{BE}$, ω_k is typically of order $k_B T$ and the typical momentum $k \approx (m_B k_B T)^{1/2}$. A typical scattering then involves a momentum transfer of $(m_B k_B T)^{1/2}$ or less. From Eqs. (4.8) and (4.9a), we see that the energy transfer ω scales as $\chi_d q^3 k_0^{-1}$ so that the typical energy transfer is $\chi_d (m_B k_T T)^{3/2} k_0^{-1} \ll k_B T$. Thus, we can make the quasielastic approximation that typically $\omega_{k'} \approx \omega_k$ and $q \approx 2k \sin(\theta/2)$. Changing the variable $\int d^2k' = m_B \int d\omega_{k'} d\theta$, we obtain

$$\Sigma_B''(k,\omega_k) \approx -\int_0^{kT} d\omega \int d\theta \frac{k_B T}{\omega} \frac{\omega (q/k_0) k^2/m_B}{\omega^2 + (\chi_d q^3/k_0)^2} , \tag{4.19}$$

where the last factor k^2 comes from the vector coupling $\mathbf{k}\cdot\mathbf{a}$. Now the ω integration can be done by scaling and, provided $kT \gg \chi_d q^3/k_0$ [which is satisfied because the rhs is approximately equal to $(kT)^{3/2}$], we obtain

$$\Sigma_B''(k,\omega_k) \approx (k_B T/m_B \chi_d) \int d\theta \frac{k^2}{q^2} . \tag{4.20}$$

The θ integral $\int d\theta [\sin(\theta/2)]^{-2}$ is again infinite from the small-θ limit. The transport time is computed in the quasielastic approximation by weighing the θ integral in Eq. (4.20) by an extra $1-\cos\theta = \sin^2(\theta/2)$. The integrand is now convergent and we obtain

$$\frac{1}{\tau_{\mathrm{tr}}^B} \approx k_B T/(m_B \chi_d) . \tag{4.21}$$

We remark that, unlike the fermion case, this result is independent of whether the clean or disordered limit is chosen in Eq. (4.9). We also note that the result that $\tau_{\mathrm{tr}}^{B\,-1}$ is proportional to $k_B T$ is a special feature of two dimensions. It has been pointed out that the boson transport scattering rate due to fermion particle-hole excitations gives a $T^{3/2}$ law.[49] Thus, the scattering due to gauge field dominates over any short-range interaction.

To emphasize the importance of gauge invariance, we derive the boson transport time in another way. We consider the boson density-density correlation function

$$\tilde{\Pi}_B = -\langle T_\tau [b^\dagger(\mathbf{r},\tau) b(\mathbf{r},\tau) b^\dagger(0) b(0)] \rangle , \tag{4.22}$$

which, unlike the boson Green function, is gauge invariant. The other gauge-invariant correlation functions of interest are the fermion density-density correlation function

$$\tilde{\Pi}_F = -\langle T_\tau [f_\sigma^\dagger(\mathbf{r},\tau) f_\sigma(\mathbf{r},\tau) f_\sigma^\dagger(0) f_\sigma(0)] \rangle \tag{4.23}$$

and the physical electron Green function

$$G_\sigma(\mathbf{r},\tau) = -\langle T_\tau [f_\sigma(\mathbf{r},\tau) b^\dagger(\mathbf{r},\tau) f_\sigma^\dagger(0) b(0)] \rangle . \tag{4.24}$$

In a space-time Feynman path formulation, Π_B is represented by a closed path in space-time which begins at $(\mathbf{r}_i,\tau_i)$ and ends at $(\mathbf{r}_f,\tau_f)$. This represents the propagation of the added particle-hole pair at $(\mathbf{r}_i,\tau_i)$ to $(\mathbf{r}_f,\tau_f)$ in a first quantized picture. In general, the added particle can exchange with existing bosons in the ground state which are represented by paths wrapping around the periodic imaginary time direction. These exchange processes can be represented by closed paths which wrap around the imaginary time axis n times. However, for $T > T_{BE}$, the exchange probability is small and we consider only the simple loop which is restricted to the domain $(0,\beta)$ in τ space. In a gauge field each path $\mathbf{r}_1(\tau)$ is weighted by $e^{i\Phi}$, where

$$\Phi[\mathbf{r}_1] = \int_{\tau_i}^{\tau_f} d\tau_1 \left[\mathbf{a}(\mathbf{r}_1(\tau_1),\tau_1)\cdot \dot{\mathbf{r}}_1(\tau_1) + a_0(\mathbf{r}_1(\tau_1),\tau_1) \right] . \tag{4.25}$$

We restrict our attention to the spatial component of the gauge field and we have seen that it is a good approximation to consider quasistatic fluctuations. Thus, we con-

sider a static but spacially varying "magnetic" field $h=\nabla\times\mathbf{a}$. In Fig. 4(a) we show the projection of a Feynman path onto real space. In the static approximation, each path is weighted by $e^{i\phi}$, where $\phi=\int\mathbf{a}\cdot d\mathbf{l}$ is the flux through the area enclosed by a loop in the projected space. To estimate h, we note that the equal-time value of

$$\langle|h_q|^2\rangle=\int\frac{d\omega}{2\pi}[n(\omega)+1]q^2\mathrm{Im}D^T(q,\omega)$$
$$\approx\frac{k_BT}{\chi_d}\quad\text{for } q<q_0\ , \tag{4.26}$$

where

$$q_0=\left[\frac{Tk_0}{\chi_d}\right]^{1/3},$$

and is small for $q>q_0$. Thus, we envision a spatially random h which varies on the scale of q_0^{-1}. The mean-square value of h can be estimated by

$$\langle h^2\rangle=\sum_q\langle|h_q|^2\rangle$$
$$\approx\frac{k_BT}{\chi_d}q_0^2\ . \tag{4.27}$$

We can write $\langle e^{i\phi}\rangle=\exp(-\frac{1}{2}\langle\phi^2\rangle)$, where $\langle\phi^2\rangle$ has contributions from patches of flux with varying signs. The flux through each patch is given by $\langle\phi_i^2\rangle=\langle h^2\rangle q_0^{-4}$ and the number of patches is Aq_0^{-2}, where A is the area of the closed loop in Fig. 4(a). We therefore conclude that

$$\langle\phi^2\rangle=Aq_0^{-2}\langle\phi_i^2\rangle=Ak_BT/\chi_d\ . \tag{4.28}$$

Note that the length scale q_0^{-1} has canceled out in this expression. Now we can write

$$\tilde{\Pi}_B=\Pi_B^0\langle e^{i\phi}\rangle\ , \tag{4.29}$$

where $\Pi_B^0=\tau^{-2}\exp(-2m_Br^2/\tau)$ is the density-density correlation function for noninteracting bosons. The free boson diffuses in imaginary time and typically $r\approx(\tau/m_B)^{1/2}$ so that typically $A\approx\tau/m_B$. Combining Eqs. (4.28) and (4.29), we see that the boson propagator has the extra decay due to the scattering by the gauge field given by the factor

$$\langle e^{i\Phi}\rangle\approx\exp[-(T/\chi_dm_B)\tau] \tag{4.30}$$

so that it is natural to interpret the lifetime $\tau_{\mathrm{tr}}=(T/\chi_dm_B)^{-1}$ as the relevant lifetime for density fluctuations. This argument, which is qualitative, has the advantage that the role of gauge invariance is clear. Only a gauge-invariant loop integral appears, which is finite, as opposed to the line integral appearing in Eq. (4.17), which is infrared divergent. Furthermore, this qualitative argument permits a generalization to strong coupling, as we shall discuss later.

A similar argument can be made for the fermion propagator $\tilde{\Pi}_F(\mathbf{r},\tau)$. The difference is that the Feynman path for a fermion on the Fermi surface is restricted to a tube of radius k_F^{-1} around the classical straight-line path. If $k_F^{-1}\ll q_0^{-1}$, the number of independent patches of fluxes is now rq_0 and the contribution from each patch is

$$\langle\phi_i^2\rangle=\langle h^2\rangle(q_0k_F)^{-2}=Tk_F^{-2}/\chi_d\ .$$

We obtain

$$\langle e^{i\phi}\rangle\approx\exp[-(T/\chi_d)^{4/3}k_Fr]\ , \tag{4.31}$$

which can be interpreted as a mean free path $l=v_F\tau_{\mathrm{tr}}^F$, where τ_{tr}^F is in agreement with Eq. (4.18).

Next we consider the physical electron Green function, Eq. (4.24). The zeroth-order calculation is to decouple this into a product of fermion and boson Green functions, which is a convolution in Fourier space.[50] The result for the spectral weight is

$$\mathrm{Im}G^R(k,\omega)$$
$$=-\int d\mathbf{q}\,\delta(\omega-\xi_{k+q}+\tilde{\omega}_q)[n(\omega_q)+f(\epsilon_{k+q})]\ , \tag{4.32}$$

where $\xi_k=\epsilon_k=\mu_F$ and $\tilde{\omega}_q=\omega_q-\mu_B$, where $\mu_B=-k_BT\ln(m_BT/2\pi x)$ is that for the free boson for $T>T_{BE}$. The first term in this expression leads to a peak centered around the energy $\epsilon_k-|\mu_B|$ with a width of order

$$\Delta\approx v_F(kTm_B)^{1/2}\ . \tag{4.33}$$

This is because the Bose factor $n(\omega_q)$ implies that the typical ω_q is of order k_BT and the typical q is of order $q_0=(k_BTmB)^{1/2}$. The δ function in Eq. (4.32) is then shifted and broadened by v_Fq_0 leading to Eq. (4.33). We note that, since $\int d\mathbf{q}n(\omega_q)=x$, the area under this peak is given by the hole concentration x.

The second term in Eq. (4.32) gives rise to a continuum with a threshold

$$\omega_c=-\frac{(k_F-|k|)^2}{2m_F}-|\mu_B| \tag{4.34}$$

which extends to $-4J$ with an area of $(1-x)/2$. We

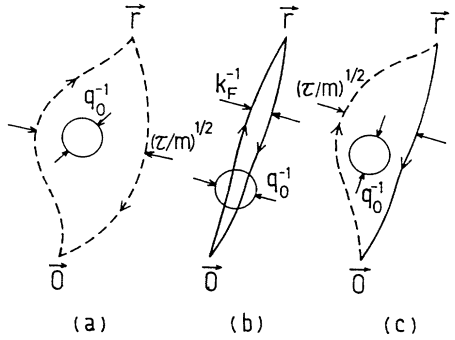

FIG. 4. Typical Feynman paths, projected onto the two-dimensional plane, which contribute to (a) the boson polarization $\tilde{\Pi}_B$, (b) the fermion polarization $\tilde{\Pi}_F$, and (c) the electron Green function G_σ. The dashed and solid lines refer to boson and fermion paths. The circle with radius q_0^{-1} represents the scale of the fluctuating gauge field flux.

note that the total area is $(1+x)/2$ instead of unity. This apparent violation of the sum rule is because our model is in the $U\rightarrow\infty$ limit and some of the spectral weight has been pushed to infinity.

We next show how this picture is modified by the coupling to the gauge field. A direct diagrammatic calculation is not feasible because, as we have seen, the self-energy corrections are infinite due to low-frequency gauge field fluctuations with $\omega<k_BT$. In principle, these infinities should be canceled by vertex corrections so that the gauge invariance of G is preserved. We have not succeeded in implementing this calculation and we resort to the following qualitative discussion. We divide the gauge field into two regimes: $\omega<T$ and $\omega>T$. For $\omega<T$ we can make the quasistatic approximation as before and compute G_σ using the path-integral method in an explicitly gauge-invariant manner. As shown in Fig. 4(c), the boson paths exhibit a random walk while the fermion path is restricted to nearly a straight line (the Gorkov approximation). We obtain

$$G=G_0\langle e^{i\phi}\rangle\approx G_0\exp[-(T/\chi_d)r(\tau/m_B)^{1/2}] .$$

Near the quasiparticle peak, we estimate the lifetime by replacing $r=v_F\tau$ in the exponent, and we obtain $\tau_{\rm in}^{-1}\approx(T/\chi_d)^{2/3}(m_Bm_F^2)^{-1/3}$. This is less than the $T^{1/2}$ width due to momentum broadening and is therefore negligible. For $\omega>T$ we can use diagrammatic methods. The calculation is convergent and essentially the zero-temperature result Eq. (4.16) applies. The dominant contribution is from the self-energy correction to the fermion, which is $J(\Omega/\chi_d)^{2/3}$. As shown in Appendix B, the first vertex correction gives rise to only logarithmic corrections. The fermion and boson have very different velocities and sample different frequency domains of the fluctuating gauge fields so that the cancellation between self-energy and vertex in the quasistatic limit no longer applies.

To summarize, $\mathrm{Im}G(\mathbf{k},\Omega)$ consists of a continuum for

$$\Omega<-|\mu_B|-(|\mathbf{k}|-k_F)^2/2m_F$$

and a peak at $\Omega=|\mathbf{k}|^2/2m_F-\mu_F$. The behavior of the spectral weight as k moves through k_F is shown in Fig. 5. The peak is severely broadened with a width equal to $\max[\Omega^{2/3}J^{1/3},(Tm_B)^{1/2}m_F^{-1}]$, which leads to an asymmetric line shape with a high-energy tail $\sim\Omega^{-2/3}$. Thus, the Landau criterion that the quasiparticle width should be less than its energy is violated. On the other hand, the location of the peak in $\mathbf{k}$ space is determined by the "spinon" Fermi surface which satisfies Luttinger's theorem. The dispersion of this peak is characterized by a bandwidth of $8J$. All these features are consistent with the photoemission data. According to our view, the observed continuum "background" is intrinsic and, in fact, contains the bulk of the spectral weight. Another interesting prediction is that, for $|\mathbf{k}|>k_F$, when the peak has moved through the Fermi surface, the continuum remains with a threshold which recedes from the Fermi energy as $|\mathbf{k}|-k_F$ increases. We also predict that the intrinsic continuum background is much reduced for inverse photoemission (BIS) or for photoemission in electron-doped materials.

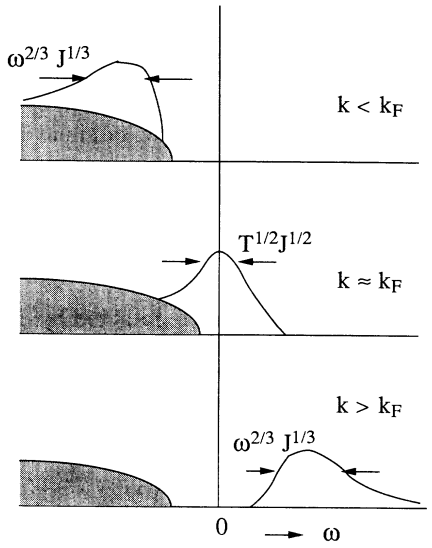

FIG. 5. Schematic drawing of the electron spectral function. The shaded area is the background and the unshaded area is a quasiparticle-like feature with area x. This feature moves through the Fermi energy ($\omega=0$) as k moves through k_F.

The tunneling density of states is readily obtained using $\Gamma(\Omega)=\int d\mathbf{k}\,\mathrm{Im}G_\sigma(\mathbf{k},\Omega)$ and we find that $\Gamma(\Omega)\sim x+|\Omega|/J$ for $\Omega<0$, but contrary to Ref. 50, $\Gamma(\Omega)\approx x$ for $\Omega>0$. This correction to Ref. 50 has already been pointed out earlier.[51] The asymmetry between particle and hole in tunneling and in photoemission is not surprising in the large-U model. An added electron can only enter a vacant site, so that for $\Omega>0$, $\mathrm{Im}G_\sigma$ and Γ are proportional to x. On the other hand, it is always possible to remove an electron so that Γ is of order unity for $\Omega<0$.

We would like to briefly comment on a phenomenological description of the normal-state properties that has been recently given by Varma *et al.*[52] Starting from the linear T dependence of the resistivity (i.e., the transport scattering rate), they hypothesized that the electron self-energy is a linear function of ω, leading to a marginal Fermi liquid. Our result shows that, in a concrete model, it is possible to obtain a linear T transport scattering rate, while at the same time the electron spectral weight has a width $\omega^{2/3}$ which violates Landau's criterion for Fermi liquid. Essentially the transport time is, in general, not necessarily the same as the electron lifetime and the hypothesis of the marginal Fermi liquid is not uniquely dictated by the transport measurements.

V. PHYSICAL QUANTITIES AND IOFFE-LARKIN COMPOSITION RULES

We are now ready to calculate various physical properties such as conductivity, Hall effect, thermopower, magnetic susceptibility, etc., including corrections due to gauge field fluctuations. Again it is important that these physical quantities are gauge invariant. This is best illus-

trated by considering the electrical conductivity, a problem first treated by Ioffe and Larkin.[26] We have to couple the physical electromagnetic field $\mathbf{A}$ to the electrons, which are now represented by $c_\sigma = f_\sigma b^\dagger$. We can couple $\mathbf{A}$ to f_σ or to $b^\dagger$ with the standard minimal coupling, but not to both and the result must be independent of this choice. By integrating out the gauge fields, Ioffe and Larkin showed that the physical conductivity σ is given by

$$\sigma^{-1} = \sigma_F^{-1} + \sigma_B^{-1} . \tag{5.1}$$

Alternatively, this result can be obtained by enforcing the constraint on the current voltage relation.[29] For concreteness let us couple $\mathbf{A}$ to the fermions. Then

$$\mathbf{J}_F = \sigma_F \boldsymbol{\epsilon}_F = \sigma_F(\mathbf{E} + \boldsymbol{\epsilon}) \tag{5.2}$$

and

$$\mathbf{J}_B = \sigma_B \boldsymbol{\epsilon}_B = \sigma_B \boldsymbol{\epsilon} , \tag{5.3}$$

where $\mathbf{E}$ and $\boldsymbol{\epsilon}$ are the electric fields corresponding to $\mathbf{A}$ and $\mathbf{a}$, respectively. The local constraint means that, on every bond, the fermion current $\mathbf{J}_F$ is opposed by a boson backflow $\mathbf{J}_B$ so that

$$\mathbf{J}_F + \mathbf{J}_B = 0 . \tag{5.4}$$

Thus, we obtain $\boldsymbol{\epsilon} = -\mathbf{E}\sigma_F/(\sigma_F + \sigma_B)$ as the average gauge field which will be produced to enforce the constraint. The physical current is $\mathbf{J} = \mathbf{J}_F = -\mathbf{J}_B$,

$$\mathbf{J} = \sigma_F \sigma_B/(\sigma_F + \sigma_B)\mathbf{E} , \tag{5.5}$$

from which Eq. (5.2) follows.

We note that

$$\sigma_B = x\tau_{\rm tr}^B/m_B \tag{5.6}$$

and $\sigma_F = (1-x)\tau_{\rm tr}^F/m_F$ so that $\sigma_F \gg \sigma_\beta$. Thus, the physical resistivity is dominated by the boson resistivity which is in agreement with experiment in both the linear T dependence and the scaling of the spectral weight with hole concentration as seen in Eq. (5.6).

The Ioffe-Larkin argument can be readily extended to other physical quantities such as the Hall effect. Here a gauge "magnetic" field h is generated in response to the physical magnetic field H, in addition to the gauge "electric" field $\boldsymbol{\epsilon}$. The gauge magnetic field h is determined by imposing the condition Eq. (5.4) on the diamagnetic currents J_F^d and J_B^d. The diamagnetic current is proportional to the magnetic field and the diamagnetic susceptibility, i.e., $J_{F,B}^d \propto \chi_{F,B} h_{F,B}$, where $h_F(h_B)$ is the magnetic field which the fermions (bosons) feel and is given by $h_F = H + h$ and $(h_B = h)$. Therefore, from Eq. (5.4), we obtain $h = -H\chi_F/(\chi_F + \chi_B)$. The Hall constant (we have adopted a convention where σ_{xy}^B is calculated for positively charged bosons) $R_H^F(R_H^B)$ is given by $\sigma_{xy}^F/(h_F\sigma_F^2)$ and $[-\sigma_{xy}^B/(h_B\sigma_B^2)]$ which is inverted to obtain an expression for σ_{xy}^F and σ_{xy}^B in terms of the Hall constant of the fermions R_H^F and bosons R_H^B, respectively. Assuming that the electric field $\mathbf{E}$ is along the x direction and the magnetic field $\mathbf{H}$ along the z direction, the currents J_x and J_y are given by

$$J_x = \sigma_{xx}E + \sigma_{xy}E_y , \tag{5.7a}$$

$$J_y = \sigma_{xy}E + \sigma_{xx}E_y , \tag{5.7b}$$

and similar expressions for the fermions and bosons, respectively. In the experimental configuration for the measurement of the Hall constant, the current $J_y = J_{Fy} = -J_{By}$ is zero which determines both ϵ_y and E_y simultaneously as $\epsilon_y = -(\sigma_B)^{-1}\sigma_{xy}^B\epsilon_B$ and $E_y = -(\sigma_F)^{-1}\sigma_{xy}^F\epsilon_F - \epsilon_y$. Putting the expressions for σ_{xy}^B, σ_{xy}^F, ϵ_B, and ϵ_F, we obtain

$$\epsilon_y = -\frac{\sigma_F\sigma_B}{\sigma_F+\sigma_B}\frac{\chi_F R_H^B}{\chi_F+\chi_B}H$$

and

$$E_y = \frac{\sigma_F\sigma_B}{\sigma_F+\sigma_B}\frac{\chi_F R_H^B + \chi_B R_H^F}{\chi_F+\chi_B}H .$$

The Hall constant R_H of the total system is the ratio $E_y/\sigma H$ and is given by

$$R_H = \frac{(R_H^F\chi_B + R_H^B\chi_F)}{(\chi_B+\chi_F)} , \tag{5.8}$$

where $R_H^F = -(1-x)^{-1}$ and $R_B = x^{-1}$ are approximated by the values for noninteracting fermions and bosons. Note that, for $T < T_{BE}$, $\chi_B \to \infty$ and we have the Fermi-liquid result $R_H \approx R_H^F$. On the other hand, for $T > T_{BE}$, using $\chi_B \approx T_{BE}/m_B T$, $\chi_F \sim (1-x)/m_F$, we conclude that the boson R_H^B dominate so that $R_H \to 1/x$ in the high-temperature limit. Experimentally the Hall number is typically a factor of 2 larger than the hole density determined by chemical means.[6] This difference was explained recently as possibly due to strong-coupling effects.[53] Experimentally R_H is found to be temperature dependent and increase with decreasing temperature. Equation (5.7) provides a mechanism for the temperature dependence of R_H via the temperature dependence of χ_B. Unfortunately, this yields an R_H which decreases with decreasing temperature, contrary to experiment. Ioffe, Kalmeyer, and Wiegmann[54] have pointed out that, in the presence of an external field, the scattering by the gauge field fluctuations becomes chiral, leading to a correction to the conductivity tensor σ_{xy}^F and σ_{xy}^B. This mechanism gives the correct sign of the temperature dependence. However, very recently Chien *et al.*[6] have successfully analyzed the temperature dependence of the Hall data in terms of a very simple model involving the introduction of an additional scattering time. It is not clear how this phenomenological model can be accommodated in the gauge field picture.

Yet another way of deriving the Ioffe-Larkin formula is by summing diagrams. For example, Π^{JJ} is obtained by summing the two terms shown in Fig. 6 and is given by

$$\begin{aligned}\Pi^{JJ} &= \tilde{\Pi}_F^{JJ} - \tilde{\Pi}_F^{JJ}(\tilde{\Pi}_F^{JJ} + \tilde{\Pi}_B^{JJ})^{-1}\tilde{\Pi}_F^{JJ} \\ &= (\tilde{\Pi}_F^{JJ\,-1} + \tilde{\Pi}_F^{JJ\,-1})^{-1} ,\end{aligned} \tag{5.9}$$

where $\tilde{\Pi}_{B,F}^{JJ}$ are the response functions which are irreducible upon cutting a single gauge field propagator. The transverse part of these functions is given by Π_F^T and Π_B^T

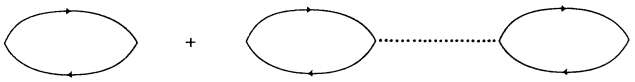

FIG. 6. A diagram for Π^{JJ} showing the screening effect of the gauge field, shown as the dotted line.

given in Eqs. (4.3) and (4.5), respectively. It should be noted that there are two limits with respect to the relative magnitude of $|\omega|$ and vq, with v being the velocity of the fermion or the boson. When $|\omega| \gg vq$, Π_F^T and Π_F^B are dominated by the first terms in Eqs. (4.3) and (4.5), respectively, and Eq. (5.9) is reduced to the composition rule Eq. (5.1) for the conductivity. In the opposite limit $|\omega| \ll vq$, Π_F^T and Π_F^B are dominated by the diamagnetic terms $\chi_F q^2$ and $\chi_B q^2$, respectively, and the orbital contribution to the magnetic susceptibility $\chi = \partial M/\partial H$ is

$$\chi^{-1} = \chi_F^{-1} + \chi_B^{-1} . \tag{5.10}$$

Since χ_B is temperature dependent, this gives rise to a temperature dependence in the physical orbital contribution to the magnetic susceptibility, which can be distinguished from the spin contribution by the anisotropy of field dependence relative to the plane. Thus, gauge theory predicts a temperature dependence in the anisotropy in the magnetic susceptibility. Experimentally there have been two reports of such anisotropy.[55,56] However, it is necessary to separate out the contribution due to superconducting fluctuations above the superconducting T_c, which complicate the analysis of the data. Ioffe and Kalmeyer[57] have discussed a fit to the data using Eq. (5.10). However, their fit seems to require a very high value of the boson mass $m_B \approx 10 m_e$ which may be inconsistent with the spectral weight of the Drude peak obtained from optical conductivity.[3]

For the density-density response function we have

$$\Pi^{\rho\rho}(q,\omega) = [\tilde{\Pi}_F(q,\omega)^{-1} + \tilde{\Pi}_B(q,\omega)^{-1}]^{-1} , \tag{5.11}$$

where $\tilde{\Pi}_{F,B}$ are the irreducible objects considered in Sec. IV. It follows that the compressibility $dn/d\mu$ is given by

$$\left[\frac{dn}{d\mu}\right]^{-1} = \left[\frac{dn}{d\mu}\right]_F^{-1} + \left[\frac{dn}{d\mu}\right]_B^{-1} . \tag{5.12}$$

The diagrammatic analysis for the off-diagonal conductivity σ_{xy} goes in a similar fashion. The diagrams for σ_{xy} contain three external vertices corresponding to E_x, E_y and H as show in Fig. 7. Each of the vertexes should be the screened one (○) represented in Fig. 8 which corresponds to the multiplication of a factor $\Pi_B^T/(\Pi_B^T+\Pi_F^T)$ to the bare vertex. For the electric vertices, the limit $|\omega| \gg vq$ should be taken and the factor is $\sigma_B/(\sigma_F+\sigma_B)$,

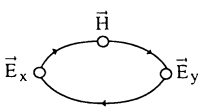

FIG. 7. A diagram for the fermionic contribution to σ_{xy}.

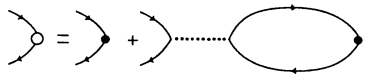

FIG. 8. The vertex screened by the gauge field.

while for the magnetic vertex the opposite limit $|\omega| \ll vq$ is relevant and the factor becomes $\chi_B/(\chi_F+\chi_B)$. This procedure results in the fermionic contribution

$$R_H^F \sigma_F^2 \frac{\chi_B H}{\chi_F+\chi_B} \sigma_B^2/(\sigma_F+\sigma_B)^2$$

to the off-diagonal conductivity σ_{xy}. The boson is not directly coupled to the external electromagnetic field, but there is a bosonic contribution through the decoration of the vertices shown in Fig. 9. The decorated vertex is $-\Pi_F^T/(\Pi_B^T+\Pi_F^T)$ times the original one. Therefore, the bosonic contribution to σ_{xy} is

$$-R_H^B \sigma_B^2 \frac{\chi_F H}{\chi_F+\chi_B} \sigma_F^2/(\sigma_F+\sigma_B)^2 .$$

Summing these fermionic and bosonic contributions, we obtain

$$\sigma_{xy} = \left[\frac{\sigma_F\sigma_B}{\sigma_F+\sigma_B}\right]^2 H \frac{\chi_B R_H^F + \chi_F R_H^B}{\chi_F+\chi_B} = \sigma^2 H R_H ,$$

which is nothing but the composition rule Eq. (5.8) for the Hall constant.

We note that this discussion does not include the modification of the gauge field propagator in the presence of the magnetic field. This has been considered by Ioffe, Kalmeyer, and Weigmann[54] who found important further temperature-dependent corrections to R_H as mentioned earlier.

Next we consider the thermopower and thermal conductivity. We can write down the linear response function for the fermion and boson systems:

$$j^\alpha = L_{11}^\alpha \epsilon^\alpha - L_{12}^\alpha \nabla T , \tag{5.13}$$

$$j_Q^\alpha = L_{21}^\alpha \epsilon^\alpha - L_{22}^\alpha \nabla T , \tag{5.14}$$

where $\alpha = F, B$, $\epsilon^F = E + \epsilon$, $\epsilon^B = \epsilon$ as before, j_α is the particle current, j_Q^α is the heat current, and

$$L_{21} = T L_{12} \tag{5.15}$$

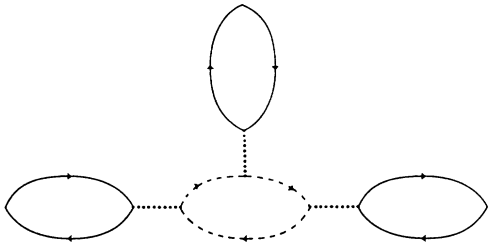

FIG. 9. A diagram for the bosonic contribution to σ_{xy}. The dashed line represents the boson propagator.

by the reciprocity relation. The thermopower $S^\alpha=\epsilon^\alpha/\nabla T=L^\alpha_{12}/L^\alpha_{11}$ is obtained by setting $j^\alpha=0$ in Eq. (5.13). For physical thermopower, we set $j=0$, which, together with the constraint $j_F+j_B=0$, implies that $j^F=j^B=0$. We can then solve for ϵ and the physical thermopower $S=E/\nabla T$:

$$S=S^F+S^B \ . \tag{5.16}$$

The thermal conductivity is obtained under the condition of zero particle current flow so that

$$\kappa^\alpha=L^\alpha_{22}-L^\alpha_{21}(L^\alpha_{11})^{-1}L^\alpha_{12} \ . \tag{5.17}$$

Writing the total heat current as $j_Q=j^F_Q+j^B_Q$ and enforcing the constraint $j^F+j^B=0$ as before, it is straightforward to show that the physical thermal conductivity $\kappa=-j_Q/\nabla T$ is given by

$$\kappa=\kappa^F+\kappa^B \ . \tag{5.18}$$

Note that, contrary to electrical conductivity, it is the thermal conductivity that adds. If we use the free-particle value for κ^F and κ^B, or alternatively, if we assume that the Wiedemann-Franz law holds for κ^α, then we expect κ to be dominated by κ^F, since $\sigma^F\gg\sigma^B$. On the other hand, the conductivity σ is dominated by σ^B so that the Wiedemann-Franz law is not expected to hold for the ratio κ/σ. Experimentally, the thermal conductivity measurement is complicated by phonon contributions and possible phonon dragg effects, but the Wiedemann-Franz law appears to hold to within a factor of 2.[58]

For free bosons we expect

$$S_B=(k_B/e)[1-\ln(2\pi x/mk_BT)]$$

so that according to Eq. (5.16) we expect S to be dominated by S_B and to be near k_B/e. Experimentally, S is approximately $0.1k_B/e$, which is much smaller than the free-boson prediction.[59] At the same time, it does not have the linear T behavior expected for Fermi liquid. There is also a report that S is much less sensitive to a large magnetic field than that expected from spin splitting effect.[60] This would support our contention that the spinless bosons dominate the thermopower. Nevertheless, the thermal transport properties κ and S are not in satisfactory agreement with the free-boson prediction. One possible solution is that the scattering by the gauge field suppresses the Bose condensation temperature and, at the same time, the normal state is not describable by a free Bose gas. However, at present, we do not have a quantitative description of such a state.

VI. SUPPRESSION OF THE BOSE-EINSTEIN CONDENSATION TEMPERATURE AND STRONG-COUPLING EFFECTS

Up to now, we have treated the boson at a temperature higher than the Bose-Einstein temperature, so that it is almost a Boltzmann gas. The dilute ideal Bose gas does not undergo a phase transition at any finite temperature, but an interacting dilute Bose gas has a transition to a superfluid phase at a temperature scale given by the Bogoliubov theory as[61,62]

$$T^{(0)}_{BE}=\frac{2\pi x c_0^{-2}}{m_B\ln\ln(1/\gamma)} \ , \tag{6.1}$$

where $\gamma=xa_0^2/c_0^2$, where c_0 is the lattice constant, a_0 is the interaction range, and Eq. (6.1) is valid in the limit $\ln\ln(1/\gamma)\gg1$. Since the double ln dependence is so weak, it appears that

$$T^{(0)}_{BE}\approx\frac{2\pi x c_0^{-2}}{m_B}\approx 4\pi x t \ , \tag{6.2}$$

where t is the hopping matrix element which corresponds to a mass of $m_B(\hbar^2/m_B=2tc_0^2)$, would serve as a reasonable characteristic energy scale for Bose condensation. Our best guess for t is that it is of order J (corresponding to $m_B\approx 2m_e$ consistent with optical measurements) which produces an estimate of $T^{(0)}_{BE}\approx 1500$ K for $x\approx 0.1$. Thus, it is very important that the true Bose condensation be suppressed to something of order 100 K in order for our theory to have any relevance to experiment at all. We have good reason to believe that the scattering of the bosons by gauge fluctuations will provide just such a mechanism for T_{BE} suppression. This is seen by the following physical agreement. The usual criterion for Bose condensation is that the de Broglie wavelength $\lambda_T=(m_BT/2\pi)^{-1/2}$ becomes comparable to the average particle spacing. The incoherent scattering by the gauge field fluctuations introduces an inelastic mean free path l. For $\tau^{-1}=\alpha k_BT$, we have $l\approx(\alpha m_BT)^{-1/2}$ and, for $\alpha>1$, l replaces λ_T as the length scale within which coherence between particles can be established and we should compare l with the interparticle spacing. This leads to a suppression of the Bose condensation temperature.

This line of argument also brings out a weakness in the perturbation theory described in Sec. IV which was based on the Boltzmann transport theory, since this theory is justified only if the mean free path l is greater than the thermal wavelength. From Eq. (4.21) we see that

$$l\approx(T/m)^{1/2}m_B\chi_d/T\approx\lambda/g \ , \tag{6.3}$$

where we have introduced the dimensionless coupling constant

$$g=(m_B\chi_d)^{-1} \ . \tag{6.4}$$

We recall that $\chi_d=\chi_F+\chi_B$ and $\chi_F\approx(1-x)/m_F$, $\chi_B\approx T^{(0)}_{BE}/Tm_B$. In the mean-field treatment of the t-J model, $m_F^{-1}\approx J$ and $m_B^{-1}\approx t$, which may be renormalized down to J. In any case, we estimate that g is of order unity near the condensation temperature and is greater than unity at higher temperatures. Thus, we need to treat the coupling to the gauge field in the strongly coupled limit. This is a difficult problem but we can make some qualitative progress in the Feynman path formulation. This was presented in Ref. 53 and here we just summarize some of the conclusions. Essentially the picture is that, in the strong-coupling limit ($g\gg1$), the important paths are no longer the diffusive loops shown in Fig. 4(a) but instead they are almost self-retracing paths. This will minimize the scattering due to the gauge field at the cost of losing some entropy. The reduction of the typical area of the

loop effectively reduces the coupling to an external magnetic field by the factor $(1+g)^{-1}$. The Landau diamagnetism is then predicted to be suppressed by

$$\chi_B = \chi_B^{(0)}/(1+g)^2 , \tag{6.5}$$

where $\chi_B^{(0)} = T_{BE}^{(0)}/m_B T$ is the susceptibility of noninteracting bosons. This can be interpreted as a suppression of T_{BE} by a factor of $(1+g)^2$ if we write $\chi_B \approx T_{BE}/mT$. Ioffe and Kalmeyer[57] have reached similar conclusions. They calculated χ_B perturbatively in an expansion in g and indeed found a reduction from $\chi_B^{(0)}$. They also did numerical studies of bosons in the presence of the random static gauge field and found that χ_B is strongly suppressed. Thus, there is good supporting evidence for the suppression of T_{BE} due to gauge field fluctuations, but a quantitative discussion is still not available.

The strong-coupling theory also improves the agreement with experiment in two ways. First, for resistivity we found a resistivity saturation phenomenon, where the boson resistivity

$$\rho_B \approx \frac{m_B T}{x} \min(g,1) . \tag{6.6}$$

For $g > 1$ this removes the temperature dependence of the coefficient of the linear term in the weak-coupling expression Eq. (4.21). Secondly, the Hall resistance is also predicted to be reduced by a factor $(1+g)$ so that $R_H^B \approx x^{-1}(1+g)^{-1}$. This may improve the agreement with the high-temperature limit of the experiment, as mentioned earlier.

The strong inelastic scattering by the gauge field may lead to a modification of the mean-field phase diagram in the following way. Besides the suppressing of T_{BE}, the onset of the pairing order parameter $D_{ij} = \langle f_{i\uparrow} f_{j\downarrow} - f_{i\downarrow} f_{j\uparrow} \rangle$ is also suppressed by the coupling to the gauge field. However, immediately below T_{BE}, a gap appears in the gauge field due to the Anderson-Higgs mechanism, and the low-frequency scattering mechanism which suppresses $T_D^{(0)}$ disappears. Thus, it is possible that pairing D_{ij} appears and the simultaneous appearance of $\langle b \rangle$ and D_{ij} means that we have a superconducting state. Similar discussion applies to the temperatures below T_D and $T_{BE}^{(0)}$ so that the boundary of the superconducting state becomes that of the thick solid line shown in Fig. 10. This provides a mechanism where there is a finite region in doping concentration where we have a transition between the strange metal phase and the superconducting phase. The Ginzburg-Landau theory for the pairing of the fermions and the bose condensation has recently been developed.[63,64] It is concluded that the only true phase transition is the superconducting one accompanied by the simultaneous appearance of $\langle b \rangle$ and D_{ij}. This is because the gauge field screens the logarithmic divergence of the single vortex energy if it remains massless. Therefore, a finite density of thermally activated vortices makes $\langle b \rangle$ or D_{ij} vanish. When the gauge field is massive, such a screening does not occur and $\langle b \rangle$ and D_{ij} can become nonzero simultaneously accompanied by the appearance of the mass of the gauge field. The nature of the superconducting state has also been discussed.[63,64]

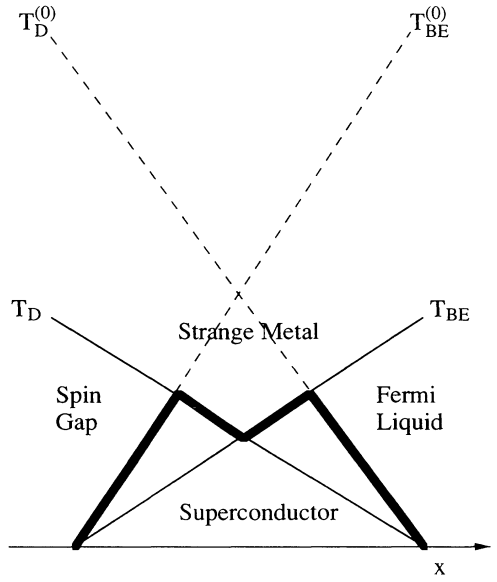

FIG. 10. Schematic illustration of the possible modification of the mean-field phase diagram shown in Fig. 1 when the inelastic lifetime effect due to gauge field fluctuations is taken into account. The thick solid line is the only genuine transition.

VII. DIRECT MEASUREMENT OF GAUGE FIELD FLUCTUATION

Since the gauge field fluctuation (or equivalent spin chirality fluctuation) plays a central role in our theory, it will be highly desirable to be able to measure it directly. The problem was addressed by Shastry and Shraiman,[65] who showed that, in a Hubbard model, the spin chirality fluctuation gives rise to Raman scattering in a geometry where the incident and outgoing polarizations are perpendicular to each other. Furthermore, they have shown how to uniquely extract the chirality contribution by adding and subtracting various scattering geometries, including linear and circular polarizations.[65] From Eq. (4.8) we predict that the Raman intensity should be

$$I(\omega,q) \propto \langle h_{q\omega} h_{-q-\omega} \rangle = \left[\frac{k_B T}{\omega} \right] q^2 \mathrm{Im} \left\{ \frac{1}{-i\omega\sigma(q) + \chi_d q^2} \right\} , \tag{7.1}$$

where q is the momentum transfer of the scattered light or the inverse of the light penetration depth, whichever is larger. We estimate $q \approx 10^4$ cm^{-1} and, if the clean limit Eq. (4.9a) is used, the characteristic Stoke's shift is $\chi_d q^3/k_0$, which is estimated to be around 2×10^4 sec^{-1}, too small to be resolved experimentally. It may be possible to measure the frequency-integrated scattered light, in which case we predict

$$\int d\omega\, I(\omega) \sim \frac{T}{\chi_d} . \tag{7.2}$$

From this experiment the temperature dependence of χ_d

can, in principle, be measured experimentally. We emphasize that our discussion is limited to low frequency. The high-frequency regime ($\omega \approx J$) is dominated by amplitude fluctuations and should be similar for doped and undoped samples. Recently, the chirality fluctuation in undoped samples at high frequency has been observed.[66]

The prospect of experimentally resolving the frequency dependence of the chirality fluctuation improves if we go away from the "strange metal" normal state. From Fig. 1 we see that there are three possibilities: (I) the overdoped regime where the bosons condense and we have a Fermi-liquid state, (II) the underdoped regime where the fermions from a pairing state and we have a spin-gap state, and (III) the superconducting regime where we have both paired fermions and condensed bosons. We can describe these three cases with a two-fluid model for the function $\sigma(q,\omega)$

$$\sigma(q,\omega)=\frac{4\pi\tilde{\rho}_s/m}{i\omega}+\tilde{\sigma}_n(q,\omega)\ , \tag{7.3}$$

where

$$\frac{\tilde{\rho}_s}{m}=\frac{\rho_s^B}{m_B}+\frac{\rho_s^F}{m_F} \tag{7.4}$$

and

$$\tilde{\sigma}_n=\sigma_n^B+\sigma_n^F\ . \tag{7.5}$$

Again, we caution that $\tilde{\rho}_s$ and $\tilde{\sigma}_n$ are not the physical superfluid density or the physical normal conductivity. In region (I), $\rho_s^B \neq 0$ and σ_n^B becomes small with decreasing temperature, but σ_n^F remains finite. In region (II), $\rho_s^F \neq 0$ and σ_n^F becomes small but σ_n^B is finite. Finally, in region (III), both ρ_s^F and ρ_s^B are nonzero and $\tilde{\sigma}_n$ is thermally activated. The main point is that, when (7.3) is substituted into Eq. (7.1), $\chi_d q^2$ effectively is replaced by ρ_s because now we have a perfect diamagnet and the energy scale of the fluctuation is greatly increased. In this case the Raman intensity is

$$I(q,\omega)=\frac{Tq^2}{4\pi\tilde{\rho}_s/m}\frac{\Gamma(q,\omega)}{\omega^2+\Gamma^2(q,\omega)}\ , \tag{7.6}$$

where

$$\Gamma=\frac{4\pi(\tilde{\rho}_s/m)}{\tilde{\sigma}_n(q,\omega)}\ . \tag{7.7}$$

Since Γ itself is frequency dependent, it cannot be simply interpreted as a width. Instead, we can make the following estimate. We parametrize

$$\tilde{\sigma}_n(q,\omega)=\frac{\sigma_0\gamma_q}{\omega^2+\gamma_q^2}\ , \tag{7.8}$$

where $\sigma_0=(\tilde{\rho}_n/m)\gamma_q^{-1}$ and γ_q is the scattering rate. We assume for simplicity that $\tilde{\rho}_n/m$ and γ_q are dominated by either the boson or fermion contribution, depending on the region (I)–(III). Then $\Gamma=(\tilde{\rho}_s/\tilde{\rho}_n)(\omega^2+\gamma_q^2)/\gamma_q$. The half-width of $I(\omega)$ depends on whether $\tilde{\rho}_s/\tilde{\rho}_n$ is large or small compared with unity. We find the half-width to be of order $\Gamma(\omega=0)=\gamma_q\tilde{\rho}_s/\tilde{\rho}_n$ for $\tilde{\rho}_s/\tilde{\rho}_n<1$ because, in this case, the assumption that Γ is ω independent is self-consistent. On the other hand, for $\tilde{\rho}_s/\tilde{\rho}_n>1$, the half-width is of order γ_q. In both cases the intensity at $\omega=0$ is $Tq^2\tilde{\sigma}_n(q,\omega=0)/(\tilde{\rho}_s/m)^2$ and vanishes when $\tilde{\rho}_n$ approaches zero.

To summarize, it is more promising to observe the Raman scattering due to chirality fluctuations in the Fermi-liquid phase, the spin-gap phase, or the superconducting phase, where the energy width is of order the fermion or boson scattering rate γ. In the superconducting phase, the scattering will vanish at low temperature as $\tilde{\rho}_n \to 0$ and the best place to look for this effect is at some intermediate temperature below, but not too far below, T_c.

VIII. CONCLUSION

We have presented a model in which a non-Fermi-liquid state emerges at a finite temperature. Chirality fluctuations described in terms of a gauge field play an important role in determining the physical properties of this state. The behavior of the single-particle Green function and the transport properties yields qualitative comparison with experiments. Recently this model has been extended to include the spin fluctuation spectrum and to compare with the nuclear spin relaxation measurement.[67] The major weakness of this model is that we do not have an adequate description of the boson system when its bose condensation temperature is suppressed by strong gauge field fluctuations. A second drawback of this model is that it is restricted to intermediate doping concentration and we have no description of how it can be connected to the antiferromagnetic state. In our theory, a spin-gap state emerges as doping is reduced, which may be in agreement with neutron and NMR experiments.[68,69] However, in our theory a gap will appear in the gauge field due to the Anderson-Higgs mechanism in the spin-gap phase and our mechanism for the linear T resistivity would disappear. It seems clear that further progress on this model requires a deeper understanding of the effect of strong coupling to the gauge field.

ACKNOWLEDGMENTS

We acknowledge support by NSF through the Material Research Laboratory program Contract No. DMR-90-22933. One of us (N.N.) also acknowledges financial support by the Monbusho International Science Research Program on "Magnetism and Superconductivity in Highly Correlated Systems."

APPENDIX A

In this appendix we evaluate the average of the one-particle Green function over gauge field fluctuations $\langle G(\mathbf{r},t)\rangle$ and show that, in two dimensions, it vanishes for any $\mathbf{r}\neq\mathbf{0}$. We use the Gorkov approximation, which states that, in a gauge field, the Green function is modified by a phase factor $G(\mathbf{r},t)=G_0(\mathbf{r},t)\exp(i\Phi)$, where

$$\Phi=\int_0^t dt_1\,\mathbf{a}[\mathbf{r}_0(t_1),t_1]\cdot\mathbf{r}_0(t_1) \tag{A1}$$

and $\mathbf{r}_0$ is a straight-line path connecting the initial and final space-time points, i.e., $\mathbf{r}_0(t_1)=\mathbf{r}t_1/t$. The average over gauge field fluctuations then reduces to a computation of $\langle \exp i\Phi \rangle$. We note that $G(\mathbf{r},t)$ is not gauge invariant so that the calculation of $\langle G(\mathbf{r},t) \rangle$ must be understood as being performed in a fixed gauge, otherwise it would trivially vanish. We fix the gauge to be the Coulomb gauge in the following.

In Fourier space we have

$$\Phi=\int_0^t \mathbf{a}\left[\frac{\mathbf{r}t_1}{t},t_1\right]\cdot\frac{\mathbf{r}}{t}dt_1$$

$$=\sum_q \int \frac{d\omega}{2\pi}\mathbf{a}_{q,\omega}\cdot\mathbf{r}\frac{e^{i(\mathbf{q}\cdot\mathbf{r}-\omega t)}-1}{i(\mathbf{q}\cdot\mathbf{r}-\omega t)} . \tag{A2}$$

Since the gauge field fluctuation is Gaussian, we obtain

$$\langle \exp i\Phi \rangle = \exp(-\tfrac{1}{2}\langle \Phi^2 \rangle) \tag{A3}$$

and

$$\langle \Phi^2 \rangle = \sum_{q,\alpha,\beta} \int \frac{d\omega}{2\pi}\langle a_\alpha(\mathbf{q},\omega)\alpha_\beta(-\mathbf{q},-\omega)\rangle \times r_\alpha r_\beta \frac{2[1-\cos(\mathbf{q}\cdot\mathbf{r}-\omega t)]}{(\mathbf{q}\cdot\mathbf{r}-\omega t)^2} . \tag{A4}$$

We can now use Eqs. (4.2), (4.8), and (4.9b), which take the form

$$\langle a_\alpha(\mathbf{q},\omega)a_\beta(-\mathbf{q},-\omega)\rangle = \cosh\left[\frac{\omega}{2k_BT}\right]\frac{\omega q}{\omega^2+Cq^6}\left[\delta_{\alpha,\beta}-\frac{q_\alpha q_\beta}{q^2}\right] , \tag{A5}$$

where C is a constant. Equation (A4) becomes

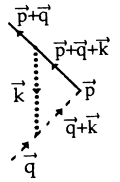

FIG. 11. The first vertex correction $\Gamma^{(1)}(p+q,p)$ for the physical electron Green function.

$$\langle \Phi^2 \rangle = \sum_q \int_0^T \frac{d\omega}{2\pi}\frac{T}{\omega}\frac{\omega q}{\omega^2+Cq^6}\left[r^2-\frac{(\mathbf{r}\cdot\mathbf{q})^2}{q^2}\right] \times \frac{2[1-\cos(\mathbf{q}\cdot\mathbf{r}-\omega t)]}{(\mathbf{q}\cdot\mathbf{r}-\omega t)^2} . \tag{A6}$$

We are interested in infrared divergences due to the small q,ω limit of the integrand, in which case

$$\langle \Phi^2 \rangle \approx \int \frac{d^2q}{(2\pi)^2}\int_0^T \frac{d\omega}{2\pi}\frac{Tqr^2/2}{\omega^2+Cq^6} \sim T\int \frac{d^2q}{(2\pi)^2}\frac{r^2}{q^2} , \tag{A7}$$

which is logarithmically divergent in two dimensions. Thus, we conclude that, for any nonzero $\mathbf{r}$,

$$\langle G(\mathbf{r},t)\rangle = G_0(\mathbf{r},t)\langle e^{i\Phi}\rangle = 0 . \tag{A8}$$

Note that our calculation has been done in a fixed gauge and $\langle G \rangle$ does not vanish in three dimensions. Thus, Eq. (A8) is not a trivial consequence of the lack of gauge invariance of the Green function.

APPENDIX B

Here we give the evaluation of the first vertex correction shown in Fig. 11. The diagram in Fig. 11 is expressed as

$$\Gamma^{(1)}(\mathbf{p}+\mathbf{q},\mathbf{q})=\frac{1}{V}\sum_{\mathbf{k}}\frac{1}{\beta}\sum_{i\omega_l}\frac{[2(\mathbf{p}+\mathbf{q})+\mathbf{k}]_\mu}{2m_F}\frac{(2\mathbf{q}+\mathbf{k})_\nu}{2m_B}\left[\delta_{\mu\nu}-\frac{k_\mu k_\nu}{k^2}\right] \times D^T(\mathbf{k},i\omega_l)G_B(\mathbf{q}+\mathbf{k},i\omega_m+i\omega_l)G_F(i\omega_n+i\omega_m+i\omega_l,\mathbf{p}+\mathbf{q}+\mathbf{k}) . \tag{B1}$$

We express $D^T(\mathbf{k},i\omega_l)$ in terms of the spectral weight as $(1/\pi)\int dx[\mathrm{Im}D^T(\mathbf{k},x)/(i\omega_l-x)]$ and we restrict ourselves to the contribution to $\Gamma^{(1)}$ from $|x|>T$, which we denote by $[\Gamma^{(1)}]_>$.

The summation over $i\omega_l$ can be done by contour integration and we obtain

$$[\Gamma^{(1)}(p+q,p)]_> = \frac{1}{V}\sum_{\mathbf{k}}\frac{1}{\pi}\int_{|x|>T}dx\frac{xk}{x^2+ck^6}\frac{(\mathbf{p}+\mathbf{q})\cdot\mathbf{q}-[(\mathbf{p}+\mathbf{q})\cdot\hat{\mathbf{k}}][\mathbf{q}\cdot\hat{\mathbf{k}}]}{m_Fm_B} \times\left\{\frac{-n_B(x)}{[i(\omega_n+\omega_m)+x-\xi_{\mathbf{p}+\mathbf{q}+\mathbf{k}}][i\omega_m-\omega_{\mathbf{q}+\mathbf{k}}]} + \frac{f(\xi_{\mathbf{p}+\mathbf{q}+\mathbf{k}})}{[i(\omega_n+\omega_m)+x-\xi_{\mathbf{p}+\mathbf{q}+\mathbf{k}}][i\omega_n-\xi_{\mathbf{p}+\mathbf{q}+\mathbf{k}}+\omega_{\mathbf{q}+\mathbf{k}}]} + \frac{n_B(\omega_{\mathbf{q}+\mathbf{k}})}{[i\omega_m+x-\omega_{\mathbf{q}+\mathbf{k}}][i\omega_n-\xi_{\mathbf{p}+\mathbf{q}+\mathbf{k}}+\omega_{\mathbf{q}+\mathbf{k}}]}\right\} . \tag{B2}$$

The absolute value of $[\Gamma^{(1)}]_>$ is bounded from above as

$$|[\Gamma^{(1)}(p+q,p)]_>| \leq \frac{1}{V}\sum_{\mathbf{k}}\frac{1}{\pi}\int_{|x|>T}dx\frac{xk}{x^2+ck^6}\frac{2(p_F+q)q}{m_F+m_B} \times\left\{\frac{|n_B(x)|}{[(\omega_n+\omega_m)^2+(x-\xi_{\mathbf{p}+\mathbf{q}+\mathbf{k}})^2]^{1/2}[\omega_m^2+(x-\omega_{\mathbf{q}+\mathbf{k}})^2]^{1/2}}\right. + \frac{f(\xi_{\mathbf{p}+\mathbf{q}+\mathbf{k}})}{[(\omega_n+\omega_m)^2+(x-\xi_{\mathbf{p}+\mathbf{q}+\mathbf{k}})^2]^{1/2}[\omega_n^2+(\xi_{\mathbf{p}+\mathbf{q}+\mathbf{k}}-\omega_{\mathbf{q}+\mathbf{k}})^2]^{1/2}} + \left.\frac{n_B(\omega_{\mathbf{q}+\mathbf{k}})}{[\omega_m^2+(x-\omega_{\mathbf{q}+\mathbf{k}})^2]^{1/2}[\omega_n^2+(\omega_{\mathbf{q}+\mathbf{k}}-\xi_{\mathbf{p}+\mathbf{q}+\mathbf{k}})^2]^{1/2}}\right\}. \tag{B3}$$

We are interested in the infrared divergence of the integral. The effective infrared cutoff is introduced by $|\omega_n|$, $|\omega_m|$, $|\omega_n+\omega_m|$, q, and the temperature T for the $\mathbf{k}$ and x integrations. The degree of the divergence is analyzed by a simple power counting. From the factor $(x^2+ck^6)^{-1}$, x scales as k^3. Considering $\xi_{\mathbf{p}+\mathbf{q}+\mathbf{k}}=\mathbf{v}_F\cdot(\mathbf{q}+\mathbf{k}+\delta\mathbf{p})$ (where $\mathbf{p}=\mathbf{p}_0+\delta\mathbf{p}$ with $|\mathbf{p}_0|=k_F$) and

$$\omega_{\mathbf{q}+\mathbf{k}}=-\mu+\frac{(\mathbf{q}+\mathbf{k})^2}{2m},$$

the $\mathbf{k}$ integration of each term of $\{\}$ in Eq. (B3) gives $\int k\,dk\cdot k(1/k\cdot k^2)$, $\int k\,dk\cdot k(1/k\cdot k)$, and $\int_0^{\sqrt{T}}k\,dk\,k(1/k^2\cdot k)$, respectively. Here the Bose factor $n_B(x)$ cannot be much larger than 1 because $|x|>T$, and the Bose factor $n_B(\omega_{\mathbf{q}+\mathbf{k}})$ restricts the integration region within the thermal wave vector $|\mathbf{k}|<(2mT)^{1/2}$. Therefore, the dominant contribution comes from the first term of $\{\}$ in Eq. (B3), which has logarithmic singularity with respect to $|\omega_n|$, $|\omega_m|$, $|\omega_n+\omega_m|$, q, and T. Therefore, we conclude that the first vertex correction gives to only logarithmic corrections.

[1]For a review of experiments, see *Physical Properties of High Temperature Superconductors II,* edited by D. M. Ginsburg (World Scientific, Singapore, 1990); and *Strong Correlation and Superconductivity,* edited by H. Fukuyaya, S. Maekawa, and A. Malozemoff (Springer-Verlag, Berlin, 1989).

[2]P. W. Anderson, Science **235**, 1196 (1987).

[3]J. Orensten *et al.,* Phys. Rev. B **42**, 6342 (1990).

[4]M. Nuss, P. M. Mankiewich, M. O'Malley, E. H. Westerwich, and P. Littlewood, Phys. Rev. Lett. **66**, 3305 (1991).

[5]D. A. Bonn, P. Dosanjh, R. Liang, and W. N. Hardy, Phys. Rev. Lett. **68**, 2390 (1992).

[6]T. R. Chien, D. A. Brawner, Z. Z. Wang, and N. P. Ong, Phys. Rev. B **43**, 6242 (1991); T. R. Chien, Z. Z. Wang, and N. P. Ong, Phys. Rev. Lett. **67**, 2088 (1991); P. W. Anderson, *ibid.* **67**, 2092 (1991).

[7]C. G. Olsen *et al.,* Phys. Rev. B **42**, 381 (1990).

[8]F. C. Zhang and T. M. Rice, Phys. Rev. B **37**, 3759 (1988).

[9]G. Baskaran, Z. Zou, and P. W. Anderson, Solid State Commun. **69**, 973 (1987).

[10]I. A. Affleck and J. B. Marston, Phys. Rev. B **37**, 3774 (1988).

[11]G. Kotliar, Phys. Rev. B **37**, 3664 (1988).

[12]I. Affleck, Z. Zou, T. Hsu, and P. W. Anderson, Phys. Rev. B **38**, 745 (1988).

[13]N. Read and S. Sachdev, Phys. Rev. B **42**, 4568 (1990).

[14]G. Kotliar and J. Liu, Phys. Rev. B **38**, 5142 (1988).

[15]M. Grilli and G. Kotliar, Phys. Rev. Lett. **64**, 1170 (1990).

[16]Menke U. Ubbens and P. A. Lee, Phys. Rev. B (to be published).

[17]P. W. Anderson, B. S. Shastry, and D. Hristopulos, Phys. Rev. B **40**, 8939 (1989).

[18]P. Wiegmann, Phys. Rev. Lett. **65**, 2070 (1990).

[19]P. Lederer, D. Poilblanc, and T. M. Rice, Phys. Rev. Lett. **63**, 1519 (1989).

[20]X. Wen, F. Wilczek, and A. Zee, Phys. Rev. B **39**, 11413 (1989).

[21]V. Kalmeyer and R. B. Laughlin, Phys. Rev. Lett. **59**, 2095 (1987).

[22]R. B. Laughlin, Science **242**, 525 (1988).

[23]R. B. Laughlin, Phys. Rev. Lett. **60**, 2677 (1988).

[24]G. Baskaran and P. W. Anderson, Phys. Rev. B **37**, 580 (1988).

[25]G. Baskaran, Phys. Scr. T **27**, 53 (1989).

[26]L. Ioffe and A. Larkin, Phys. Rev. B **39**, 8988 (1989).

[27]N. Nagaosa and P. A. Lee, Phys. Rev. Lett. **64**, 2450 (1990).

[28]L. Ioffe and P. Wiegmann, Phys. Rev. Lett. **65**, 653 (1990).

[29]L. Ioffe and G. Kotliar, Phys. Rev. B **42**, 10348 (1990).

[30]S. E. Barnes, J. Phys. F **6**, 1375 (1976).

[31]P. Coleman, Phys. Rev. B **29**, 3035 (1984).

[32]N. Read and D. Newns, J. Phys. C **16**, 3272 (1983).

[33]D. Arovas and A. Auerbach, Phys. Rev. B **38**, 316 (1988).

[34]B. Shraiman and E. Siggia, Phys. Rev. Lett. **62**, 1564 (1989).

[35]D. Yoshioka, J. Phys. Soc. Jpn. **58**, 32 (1989); **58**, 1516 (1989).

[36]C. L. Kane, P. A. Lee, T. K. Ng, B. Chakraborty, and N. Read, Phys. Rev. B **41**, 2653 (1990).

[37]C. Jayaprakash, H. R. Krishnamurthy, and S. Sarker, Phys. Rev. B **40**, 2610 (1989).

[38]J. B. Marston and I. Affleck, Phys. Rev. B **39**, 11538 (1989).

[39]T. Dombre and G. Kotliar, Phys. Rev. B **39**, 855 (1989).

[40]P. Wiegmann, Phys. Rev. Lett. **60**, 821 (1988); Physica C **153-155**, 103 (1988).

[41]X. G. Wen, Phys. Rev. B **39**, 7223 (1989).

[42]P. A. Lee, Phys. Rev. Lett. **63**, 680 (1989).

[43]R. Shankar, Phys. Rev. Lett. **60**, 203 (1989).

[44]D. Poilblanc, E. DaGotto, and J. Riera, Phys. Rev. B **43**, 7899 (1991).
[45]See D. Pines and P. Nozieres, *The Theory of Quantum Liquid* (Benjamin, New York, 1966), p. 182.
[46]T. Holstein, R. Norton, and P. Pincus, Phys. Rev. B **8**, 2649 (1973).
[47]M. Reizer, Phys. Rev. B **39**, 1602 (1989).
[48]For a review, see B. L. Altshuler and A. G. Aronov, in *Electron-Electron Interaction in Disordered Systems,* edited by A. L. Efros and M. Pollak (Elsevier Science, New York, 1985), p. 1.
[49]K. Kallin and J. Berlinsky, Phys. Rev. Lett. **60**, 2526 (1988).
[50]P. W. Anderson and Z. Zou, Phys. Rev. Lett. **60**, 132 (1988).
[51]K. Flemsberg, P. Hedegard, and M. Pedersen, Phys. Rev. B **38**, 841 (1988).
[52]C. M. Varma, P. B. Littlewood, S. Schmitt-Rink, E. Abrahams, and A. Ruckenstein, Phys. Rev. Lett. **63**, 1996 (1989).
[53]N. Nagaosa and P. Lee, Phys. Rev. B **43**, 1233 (1991).
[54]L. B. Ioffe, V. Kalmeyer, and P. B. Wiegmann, Phys. Rev. B **43**, 1219 (1991).
[55]M. Miljak, G. Gollin, A. Hamzic, and V. Zlatic, Europhys. Lett. **9**, 723 (1989).
[56]R. E. Walstedt, R. F. Bell, L. F. Schreemeyer, J. V. Waszczak, and G. P. Espinosa (unpublished).
[57]L. B. Ioffe and V. Kalmeyer, Phys. Rev. B **44**, 750 (1991).
[58]S. J. Hagen, Z. Z. Wang, and N. P. Ong, Phys. Rev. B **40**, 9389 (1989).
[59]M. Sera, S. Shamoto, and M. Sato, Solid State Commun. **68**, 649 (1988).
[60]R. C. Yu *et al.*, Phys. Rev. B **37**, 7963 (1988).
[61]V. N. Popov, Theor. Math. Phys. **11**, 565 (1972).
[62]D. S. Fisher and P. C. Hohenberg, Phys. Rev. B **37**, 4936 (1988).
[63]S. Sachdev, Phys. Rev. B **45**, 389 (1992).
[64]N. Nagaosa and P. A. Lee, Phys. Rev. B **45**, 966 (1992).
[65]B. S. Shastry and B. Shraiman, Phys. Rev. Lett. **65**, 1068 (1990); Int. J. Mod. Phys. B **5**, 365 (1991).
[66]P. Sulewski, P. A. Fleury, K. B. Lyons, and S. W. Cheong, Phys. Rev. Lett. **67**, 3864 (1991).
[67]T. Tanamoto, K. Kuboki, and H. Fukuyama, J. Phys. Soc. Jpn. **60**, 3072 (1991).
[68]J. Rossat-Mignod *et al.* (unpublished).
[69]For a review, see R. Walstedt and W. Warren, Science **248**, 1082 (1990).

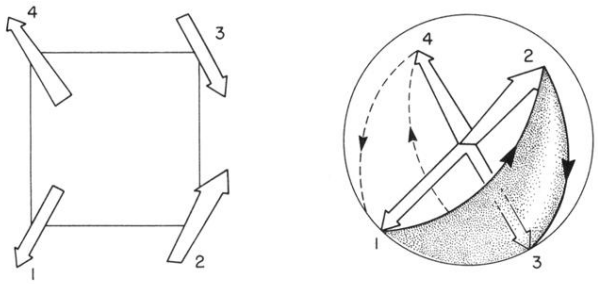

FIG. 2. (a) Four sites around a square plaquette with an instantaneous spin configuration. The spin on site 2 points out of the plane while the spin on site 4 points into the plane. (b) The tip of the unit vectors representing the instantaneous spin orientation shown in (a) are put on the surface of a sphere. In this example, spin 2 is on the front hemisphere while spin 4 is on the rear hemisphere. The path 1234 traces out a solid angle which can be interpreted as the gauge flux through the plaquette. Note that, if spins 2 and 4 both point out of the plane, the solid angles formed by 123 and 341 will have opposite sign and tend to cancel each other.

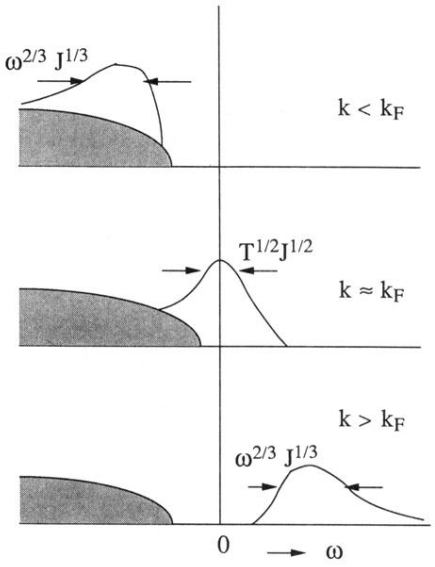

FIG. 5. Schematic drawing of the electron spectral function. The shaded area is the background and the unshaded area is a quasiparticle-like feature with area x. This feature moves through the Fermi energy ($\omega=0$) as k moves through k_F.